

**PHOTOACOUSTIC DETECTION AND SPECTRAL  
ANALYSIS OF HEMOZOIN IN HUMAN LEUKOCYTES  
AS AN EARLY INDICATOR OF MALARIA INFECTION**

---

A Thesis presented to the Faculty of the Graduate School  
University of Missouri

---

In Partial Fulfillment  
Of the Requirements for the Degree

Master of Science

---

by

JONATHAN RYAN CUSTER

Dr. John A. Viator, Thesis Supervisor

DECEMBER 2011

© Copyright by Jonathan R. Custer 2011  
All Rights Reserved

The undersigned, appointed by the Dean of the Graduate School, have examined the thesis entitled:

**PHOTOACOUSTIC DETECTION AND SPECTRAL  
ANALYSIS OF HEMOZOIN IN HUMAN LEUKOCYTES  
AS AN EARLY INDICATOR OF MALARIA INFECTION**

Presented by Jonathan R. Custer

A candidate for the degree of Master of Science

And hereby certify that in their opinion it is worthy of acceptance.

---

Dr. John A. Viator  
Biological Engineering

---

Dr. Brenda T. Beerntsen  
Veterinary Pathobiology

---

Dr. Gang Yao  
Biological Engineering

This Work Is Dedicated To My Mother  
Brenda Jobe Custer

## ACKNOWLEDGEMENTS

I spent the large majority of my life believing that if you want something done right then you have to do it yourself. Not only is this old adage extremely ego-centric, its downright wrong. Through the course of my education at the University of Missouri I have learned that without the help of your peers and colleagues accomplishing the required coursework and pushing the boundaries of scientific advancement is an insurmountable task. I would like to personally acknowledge Dr. John A. Viator, my advisor, mentor, and friend. Dr. Viator saw potential in me where others did not. Through his wisdom and ingenuity he proposed a project of significant magnitude. He entrusted this project to me, and had faith that I would accomplish what needed to be done. He proposed a novel method for detection of malaria within infected individuals. Without his creativity and vision, this project would have never existed, or succeeded. I would like to once again thank Dr. Viator personally for his support and dedication.

Secondly, I must thank Professor Brenda T. Beerntsen of the Veterinary Pathobiology Department. She has supplied me with a space to conduct much of my research. Her facilities and helpful students were instrumental in the success of this work. Also, I would like to thank Dr. Michael Kariuki for bestowing upon me his knowledge of cellular culturing techniques, and the donation of his valuable time. Other students of Dr. Beerntsen, Renee Roberts and Maggie Schlarman, have made innumerable contributions to this work. They have always graciously donated their time for anything that I could have needed, whether it was helping in the preparation of reagents, sharing their malaria cultures, answering questions about the nature of malaria culturing, or simply sharing their lab space.

I would also like to personally thank Benjamin Goldschmidt for all of his help. He was never shy to help answer any questions I had about the lab, or any equipment I may have been unfamiliar with. He helped with setting up the laser on numerous occasions. He also offered intellectual insight on my project and offered suggestions on how to improve results. He was always available and always made time for

me, or any student, who needed his expertise. The personal attention that Kiran Bhattacharyya gave to me, as well as other students, should also be acknowledged. He showed me a simple method for aligning the optical fiber, and also offered his insight into methods that could increase the accuracy of my experiments.

Christine OBrien dedicated time and patience to help fine tune the photoacoustic malaria detection system. She worked many long nights along side of me. She donated her expertise into the workings of a two phase flow detection and isolation system. She helped in the construction of our paper to document the success of a two phase flow malaria detection apparatus. Without her, this project would have ultimately resulted in failure. There are not words that can accurately express my appreciation of her contributions.

I wish to thank the Biological Engineering Department of the University of Missouri-Columbia, specifically Dr. Gang Yao for serving on my thesis committee. In addition I would like to acknowledge Dr. Yao for instilling upon me the knowledge of light and tissue interactions, as well as conveying the knowledge of other optical properties and techniques. I also have much appreciation for Dr. Steven Borgelt, he has served as a personal mentor and has always helped me to maintain grounded in this fast paced academic environment. I certainly cannot forget the assistance of Dr. Sheila Grant. It was thanks to her that I started doing research at the University of Missouri. She allowed me to work in her lab, where I was able to characterize the properties of explanted hernia mesh materials through the observance of changes in their optical properties. Through the use of FT-IR spectroscopy I was able to determine characteristic changes in explanted hernia materials compared to their pristine counterparts. It was through this experience that I became interested in researching optical properties of materials.

Finally, I would to thank my family for their tireless support. My mother, Brenda Jobe Custer has been an infinite source of inspiration. She sacrificed her career in order to be the best mother that she could be. I could not have asked for a better role model. My father, Neil Custer, was the one who steered me in the direction of studying Biological Engineering and without that direction I would have never

ended up where I am today. My sister, Dr. Jamie Lynn Custer, has been a source of inspiration and competition since childhood. Always trying to outdo the other, we pushed each other to significant heights.

# TABLE OF CONTENTS

<b>ACKNOWLEDGEMENTS.....</b>	<b>ii</b>
<b>LIST OF FIGURES.....</b>	<b>vi</b>
<b>ABSTRACT.....</b>	<b>viii</b>
<b>CHAPTER</b>	
<b>1 BACKGROUND AND INTRODUCTION . . . . .</b>	<b>1</b>
1.1 Malaria . . . . .	1
1.1.1 History . . . . .	1
1.1.2 Malaria and its Effects on the Modern World . . . . .	2
1.1.3 Biology of Plasmodium Falciparum . . . . .	3
1.1.4 Current Diagnosis and Treatment . . . . .	6
1.2 The Photoacoustic Effect . . . . .	7
1.2.1 History . . . . .	7
1.2.2 Theory . . . . .	8
1.2.3 Current Research and Applications . . . . .	10
<b>2 INITIAL DESIGN AND IMPLEMENTATION . . . . .</b>	<b>12</b>
2.1 Specific Aims and Goals . . . . .	12
2.2 Parasite Culturing . . . . .	12
2.2.1 Blood . . . . .	13
2.2.2 Media . . . . .	13
2.2.3 Culture Preparation . . . . .	14
2.2.4 Biology of White Blood Cells . . . . .	14
2.2.5 Monocyte Isolation and Addition . . . . .	15
2.3 Initial Photoacoustic Tests . . . . .	17
2.3.1 Acrylamide Well Preparation . . . . .	17
2.3.2 Piezoelectric Transducer Manufacturing . . . . .	21
2.3.3 Acrylamide Well Tests . . . . .	21



2.3.4	Initial Flow system Tests . . . . .	26
2.3.5	Tween 80 Surfactant Experiment . . . . .	27
<b>3</b>	<b>FINAL SYSTEM DESIGN . . . . .</b>	<b>35</b>
3.1	Abstract . . . . .	35
3.2	Introduction . . . . .	35
3.3	Materials and Methods . . . . .	38
3.3.1	Leukocyte Laden Blood . . . . .	38
3.3.2	Pigment Containing Leukocytes . . . . .	39
3.3.3	Flow Chamber Design . . . . .	40
3.3.4	Two Phase Photoacoustic Detection and Isolation . . . . .	41
3.3.5	Single Phase Photoacoustic Spectral Analysis . . . . .	43
3.4	Results . . . . .	44
3.4.1	Pigment Containing Leukocytes . . . . .	44
3.4.2	Two-Phase Photoacoustic Detection and Isolation . . . . .	47
3.4.3	Photoacoustic Spectral Analysis . . . . .	47
3.5	Discussion . . . . .	49
<b>4</b>	<b>GENERAL DISCUSSION AND CONCLUSIONS . . . . .</b>	<b>54</b>
4.1	Photoacoustic Detection System . . . . .	54
4.2	Pigment Containing Leukocyte Detection . . . . .	55
4.3	Future Directions . . . . .	56
4.4	Conclusion . . . . .	56
	<b>BIBLIOGRAPHY . . . . .</b>	<b>58</b>

## LIST OF FIGURES

<b>Figure</b>	<b>Page</b>
1.1 Anopheles Mosquito . . . . .	3
1.2 Erythrocytic Life Cycle . . . . .	5
2.1 Image of the Well Housing . . . . .	18
2.2 Acrylamide Solution After Being Poured Into the Well Housing . . .	19
2.3 Image of the Well After it Has Solidified . . . . .	20
2.4 Top View of the Piezoelectric Transducer . . . . .	22
2.5 Side view of the piezoelectric transducer . . . . .	23
2.6 Model of Original Photoacoustic Setup . . . . .	24
2.7 Data Obtained From Original Photoacoustic Setup . . . . .	25
2.8 Preliminary Two Phase Flow Data . . . . .	28
2.9 Post Excitation Resultant Data . . . . .	29
2.10 Tween 80 Static Photoacoustic Response . . . . .	32
2.11 Final Two Phase Flow Photoacoustic Response . . . . .	34
3.1 PCL Histopaque 1119 Isolation . . . . .	40
3.2 Schematic of Photoacoustic Flow System from Side and Top Views .	43
3.3 Orthogonal View of the Detection Chamber . . . . .	44
3.4 Free Hemozoin as Indicated By Arrow . . . . .	45
3.5 Pigment Containing Leukocyte as Indicated By Arrow . . . . .	46
3.6 530 nm Photoacoustic Waveform . . . . .	48
3.7 Captured Post Excitation PCL . . . . .	49
3.8 Photoacoustic Spectral Analysis . . . . .	50
3.9 Combining Two Immiscible Fluids Into One Flow Path in a Microfluidic System . . . . .	51

# PHOTOACOUSTIC DETECTION AND SPECTRAL ANALYSIS OF HEMOZOIN IN HUMAN LEUKOCYTES AS AN EARLY INDICATOR OF MALARIA INFECTION

Jonathan Ryan Custer

Dr. John A. Viator, Thesis Supervisor

## ABSTRACT

Malaria is a blood borne infection affecting hundreds of millions of people worldwide. The parasites that cause this disease reproduce within the red blood cells, eventually causing their death and lysis. This process releases the parasites into the blood, continuing the cycle of infection. Usually, malaria is diagnosed only after a patient presents symptoms, including high fever, nausea, and, in advanced cases, coma and death. While reproducing within the bloodstream of a host, malaria parasites convert hemoglobin into an insoluble crystal, known as hemozoin. These crystals, approximately several hundred nanometers in size, are contained within red blood cells and white blood cells that ingest free hemozoin in the blood. Thus, infected red blood cells and white blood cells contain a unique optical absorber that can be detected in blood samples using photoacoustic detection methods. Our group separated the white blood cells from malaria infected blood and tested it *in vitro* using a photoacoustic set up with a tunable laser system consisting of an optical parametric oscillator pumped by an Nd:YAG laser with pulse duration of 5 ns. These cells were tested at multiple wavelengths, and results imply the potential to assay simple blood draws from healthy and infected patients for the presence of hemozoin, thus providing a novel method for the indication of malaria infection.

# Chapter 1

## Background and Introduction

### 1.1 Malaria

#### 1.1.1 History

Evidence of the existence of malaria parasites has been found preserved within mosquito fossils from 30 million years ago (Poinar, 2005), thus malaria has plagued mankind since antiquity, growing and evolving along with the human species. Some sources believe that the malaria parasitic infection has been present during the entire duration of the human species (Joy *et al.*, 2003). Unique references to periodic unexplained fevers can be found referenced throughout history. Many of these were attributed to demons or spirits, and were commonly treated with holistic medical approaches such as bloodletting. In ancient Greece scholars thought that the disease was caused by miasma. Miasma was believed to be some form of noxious pollution carried in the air and dispersed by the winds. The name malaria was actually derived from Mal Aria, which means bad air in the medieval Italian language. The disease was often called marsh fever, as per its association with swamps and marshlands (Reiter, 2000).

The cause of human malaria, the parasite *Plasmodium falciparum*, was discovered in 1880 by a French army doctor who worked in a military hospital. It was here that Charles Louis Alphonse Laveran observed the parasites for the first time, inside the red blood cells of people suffering from the disease. He proposed that malaria was caused by this organism. It was the first time a protist was identified as being a disease causing agent (Nye, 2002).

In 1898 Sir Ronald Ross proved that malaria was transmitted by mosquitoes. He showed that malaria could be transmitted to certain birds by several species of mosquito. He then isolated the malaria parasites within the salivary glands of the

mosquitoes in question that fed on these birds (Nye & Gibson, 1997). It was later discovered that mosquitoes of the genus *Anopheles* transmit the disease to humans. Both Ross and Laveran earned Nobel prizes for their work in demonstrating the communicability and cause of the disease.

### 1.1.2 Malaria and its Effects on the Modern World

Malaria has been one of the most destructive socioeconomic forces of the modern age. For centuries malaria has outranked warfare as a source of human suffering. Over the past generation it has killed millions of human beings and sapped the strength of hundreds of millions more. It continues to be a heavy drag on mans efforts to advance his agriculture and industry (WHO, 2011). John F. Kennedy was quoted as saying, Indeed, malaria has played an important role in the rise and fall of nations and has killed untold millions the world over (WHO, 2011).

Despite efforts from a multitude of nations to eradicate malaria and the vectors that bare it, malaria still remains one of the most impacting diseases on the planet in terms of lives lost and economic burden. Elimination of malaria in an area does not require the elimination of all *Anopheles* mosquitoes capable of transmitting the disease. In North America and Europe, *Anopheles* mosquitoes capable of transmitting malaria are still present, but the parasite has been eliminated. Socioeconomic improvements (e.g., houses with screened windows, air conditioning) combined with vector reduction efforts and effective treatment have led to the elimination of malaria without the complete elimination of the vectors (CDC, 2011).

Nearly 3.3 billion human beings live in regions of the world where malaria is endemic, meaning that both the parasites that cause the disease, as well as the vectors that bear the disease are present. There are approximately 250 million cases of malaria contracted annually resulting in the loss of approximately 1 million lives, most of which belong to sub-Saharan African youth (WHO, 2011). The malaria parasite is borne by the mosquito of the genus *Anopheles*. Nearly 40 different species of the aforementioned genus can transmit the disease. These species inhabit the majority of human populated regions. While the disease is not always present in



Figure 1.1: Anopheles Mosquito

the same areas as the vector, there is a chance that the parasite could spread into other regions than it currently inhabits, i.e. the United States (Zucker, 1996).

### 1.1.3 Biology of Plasmodium Falciparum

Malaria is caused by infection from a blood borne eukaryotic protist of the genus *Plasmodium*. There are three main species of the *Plasmodium* parasites that infect humans: *P. vivax*, *P. ovale*, and *P. falciparum*. *P. falciparum* is the most damaging to humans. Its symptoms include, but are not limited to, high fever, chills, nausea, sweats, muscle aches, tiredness, anemia, jaundice and, in advanced cases, kidney failure, seizures, coma, and death (CDC, 2011). The symptoms caused by *P. vivax* and *P. ovale* are similar, but often much less severe. *P. falciparum* is the most prevalent species of plasmodium accounting for a majority of all malarial infections (WHO, 2011). *P. falciparum* has two distinct phases of its life cycle: the invertebrate stage and the vertebrate stage. The invertebrate stage of the parasite exhibits sexual reproduction, much different than the asexual reproduction exhibited in the erythrocytic life cycle.

The invertebrate stage of the parasites life cycle begins when an *Anopheles* mosquito takes a blood meal from an infected human. The mosquito unknowingly ingests a form of the parasite known as a gametocyte. The gametocyte is a

differentiation of the parasites normal vertebrate life cycle. There are two types of gametocytes that develop, macrogametes and microgametes. After an indeterminate number of erythrocytic life cycles the parasite begins to develop these gametocytes (Roberts & Janovy, 2008). When these gametocytes are ingested by the mosquito they develop into gametes. The macrogametocytes mature into a macrogamete. The microgametocytes undergo a transformation in which they develop flagella. These flagellate microgametes travel about until they find a macrogamete, in which they penetrate and fertilize.

The zygote that forms from this sexual reproduction elongates and becomes what is known as a motile ookinete (Roberts & Janovy, 2008). The aforementioned ookinete migrates to the gut of the mosquito. It penetrates the cellular wall of the gut and begins to transform into an oocyst. The oocyst differentiates into a form called a sporoblast. These sporoblasts divide rapidly into thousands of sporozoites (Roberts & Janovy, 2008). These sporozoites break out of the oocyst and migrate through the mosquito until they enter the salivary glands. At this point the mosquito is now infective. Once a mosquito is infected with the parasite it remains infective for the duration of its life. This process of becoming infective takes approximately 10-14 days (Roberts & Janovy, 2008).

The vertebrate stage of the parasites life cycle begins with the bite from an infective female *Anopheles* mosquito. When the bite is initiated the mosquito injects its saliva into the host organism in order to numb the tissue so that it may feed undisturbed. However, a mosquito that is infected with *P. falciparum* will unknowingly inject sporozoites carried within the saliva. These sporozoites, which are about 1  $\mu\text{m}$  in diameter and 10-15  $\mu\text{m}$  in length (Roberts & Janovy, 2008), travel through the blood stream where they are deposited in the liver. In the liver, they invade the hepatic cells. During the next 10-14 days the sporozoites differentiate and undergo schizogony, a form of asexual reproduction in which multiple mitoses take place, followed by simultaneous cytokinesis, resulting in many daughter cells at once (Roberts & Janovy, 2008). These daughter cells are called merozoites. Upon lysis of the hepatic cells thousands of merozoites are released

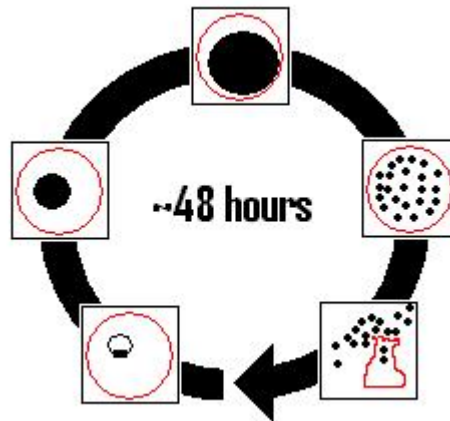


Figure 1.2: Erythrocytic Life Cycle

into the blood stream where they begin to invade the host erythrocytes (red blood cells). This invasion of the host erythrocytes marks the beginning of *P. falciparum*'s asexual erythrocytic reproductive cycle. Upon entry into the host erythrocytes the merozoites differentiate into trophozoites. Initially, host cytoplasm ingested by the trophozoite forms a large food vacuole, which gives the parasite a ring-like appearance where-in the nucleus lies along the outer circumference of the ring when examined with light microscopy. As the parasite grows in size, the appearance of the food vacuole becomes less apparent. However, hemozoin crystals begin to aggregate and become visible in the food vacuole. Hemozoin is the byproduct of *P. falciparum*'s consumption of the hosts hemoglobin within the erythrocyte. When the trophozoite is mature it undergoes schizogony, thus rapidly developing into a schizont. This schizont houses 8-20 merozoites. Once the merozoites are mature, the erythrocyte ruptures, thus releasing the merozoites, as well as metabolic wastes, including hemozoin. The merozoites are then free to invade new erythrocytes and the process repeats itself approximately every 48 hours. This process is diagramed in Figure 1.2.

During the trophozoite stage of the *Plasmodium* life cycle, parts of the erythrocyte are consumed by the parasite. Nearly 90% of the protein contained



within the erythrocyte is contributed by the hemoglobin (Jani *et al.*, 2008). During the metabolic breakdown of hemoglobin, large quantities of heme are released. This heme is toxic to biological cells and the parasite utilizes a novel mechanism where it rapidly converts heme into a crystalline material known as hemozoin (Jani *et al.*, 2008). Hemozoin is an insoluble crystalline polymer which has unique optical absorbance properties. This optical absorber can be found free floating in the blood stream of subjects who exhibit malarial infection. This polymer can also be found within erythrocytes where *P. falciparum* is incubating, as well as within host leukocytes (white blood cells).

#### 1.1.4 Current Diagnosis and Treatment

The most prevalent method for malaria detection is the same as how the parasite was discovered in the first place, microscopic analysis of infected blood cells (Krafts *et al.*, 2011). Thick blood smears are used to determine the presence of parasites within the hosts blood, which is usually obtained through a finger prick. If the presence of any parasites is determined then a thin blood film can be observed in order to determine which species of malaria is present. There is much debate as to the efficacy of microscopic diagnosis. The World Health Organization says that a skilled microscopist can detect between 5-20 parasites per  $\mu\text{L}$  of blood (WHO, 2011). However, studies show that these diagnosis could be accurate only 71% of the time (Ohrt *et al.*, 2002; Milne *et al.*, 1994)

Another method of detection currently being utilized is the use of malaria rapid antigen tests. These tests are commercially available and require only a drop of blood to test for the presence of malaria parasites. They can be advantageous for use in non-endemic regions, as skilled microscopists may be unavailable. The tests take approximately 15-20 minutes to give an indication of infection. They are sensitive to around 100 parasites/ $\mu\text{L}$ . However, a skilled microscopist can detect infection with a higher efficacy, and in about the same amount of time. Another disadvantage of the rapid antigen tests is their cost, and their qualitative nature. They can indicate the presence of parasites, but not the level of parasitemia. Currently the best treatment

for malaria is prevention. This can be accomplished through many means including but not limited to anti-malarial drugs, such as doxycycline, vector control efforts, and malaria nets. However, if malaria is contracted it is typically treatable. The most common and widely used medication for the treatment of malaria was, in the past, chloroquine. However, *P. falciparum* has become widely immune to this treatment, most likely due to its overuse in non-infected patients (Uhlemann & Krishna, 2005; Savarino *et al.*, 2003). In areas where malaria diagnosis is unavailable, the presence of fever was subsequently treated with this anti-malarial regardless of a laboratory diagnosis, this is could have caused the widespread development of immunity.

## 1.2 The Photoacoustic Effect

### 1.2.1 History

The photoacoustic effect is a well documented phenomenon wherein light is used to create pressure waves. The photoacoustic response of materials has been known for over 100 years. Alexander Graham Bell discovered this effect while trying to wirelessly convey audible tones in 1881. He called his device called the Phonophone. This device utilized intermittent pulses of focused sunlight upon thin disks of various materials to create audible sound waves that could be received with a hearing tube (Bell, 1881). These pulses were created using a slotted rotating disk. He noted that the frequency and amplitude of the sounds generated varied with the intensity and frequency of the light source. His discovery was mostly thought of as a curiosity at the time of its development and was largely unexplored for a number of years. Following the advent of the microphone, which enabled more accurate monitoring of acoustic waves, Bell's research into photoacoustics was rekindled by M. L. Viengerov in the late 1930s. Viengerov performed photoacoustic experiments on gases, namely carbon dioxide and nitrogen. He was able to measure concentrations accurately within .2% by volume (Rosencwaig, 1980). This remained the most used application of photoacoustic techniques for the next several decades. With the advent of high intensity laser light and sensitive transducer elements, photoacoustics have made

significant advances in the last several decades. Photoacoustics offer a means of measuring optical properties and responses much different from current optical techniques. The majority of current optical techniques measure absorbance and scattering of light directly upon a media of interest. Photoacoustics offer a means of indirectly measuring the responses of materials to optical excitation.

### 1.2.2 Theory

Modern photoacoustics are much different than the general principles discovered by Alexander Graham Bell. Modern photoacoustics utilize high energy, sub  $\mu\text{s}$  pulse duration, laser light to induce ultrasound acoustic pressure waves. The field of photoacoustics studies pressure waves created by intermittent light energy applied to an analyte of interest. These analytes are typically some form of chromophore. A chromophore is the part of a substance or molecule that is responsible for the visible color of the substance. The visible color is determined by the optical absorption properties of the chromophore. Certain wavelengths of light are absorbed, and some are reflected and scattered. The reflected portions of light are what we can visibly detect, while the absorbed wavelengths are not reflected. These chromophores can also absorb non-visible spectrums of light, including infrared and ultraviolet. An inherently red chromophore will thus give a small photoacoustic response when red light is applied to it, as much of the energy will not be absorbed. However, if a wavelength of higher absorbance is applied to the chromophore an inherent photoacoustic response can be measured. The acoustic pressure waves are generated based on each chromophores thermo-elastic properties. When energy is absorbed by a photon excited chromophore, the optical energy is converted into thermal energy that becomes trapped within the chromophore. Thus, subsequent thermoelastic expansion develops. Thermoelastic expansion can be described as energy that is quickly absorbed by a chromophore such that the resulting localized heating causes rapid expansion of the chromophore that proliferates as pulse of acoustic energy (Viator *et al.*, 2004) Thermoelastic expansion occurs when the condition of stress confinement is achieved by depositing energy directly into a chromophore in a

manner such that the energy is unable to propagate away acoustically and must therefore be absorbed as localized convection (Viator *et al.*, 2004). This condition is expressed in Equation 1.1

$$t_p < \delta/c_s \quad (1.1)$$

In this equation  $t_p$  is the laser pulse duration,  $\delta$  is the absorption depth of laser energy, and  $c_s$  is the speed of sound in the medium (Paltauf *et al.*, 1996).

Rapid thermoelastic expansion can be obtained by exciting an optically absorbing analyte with transient pulses of laser light. This will result in subsequent expansion and contraction of the chromophore causing radial pressure waves traveling away from the analyte. When greater amounts of energy are absorbed subsequently greater amounts of heat are produced, thus an increase in the magnitude of the pressure wave is observed. This thermoelastic expansion that results in the production of ultrasonic pressure waves can be described by Equation 1.2

$$p(z) = \frac{1}{2}\mu_a\Gamma e^{-\mu_a z} \quad (1.2)$$

In this equation  $p(z)$  represents pressure at depth  $z$ ,  $\mu_a$  is the optical absorption coefficient of the tissue, and  $\Gamma$  is the Gruneisen coefficient, which denotes the fraction of optical energy converted into kinetic energy in the form of ultrasonic pressure waves. This coefficient is temperature dependent and is equal to 0.12 at room temperature for most tissue. This equation assumes that the chromophore is a pure optical absorber in which  $\delta = 1/\mu_a$  (Viator *et al.*, 2002; Viator *et al.*, 2004; Paltauf *et al.*, 1996).

Equation 1.2 shows that the amount of photoacoustic response observed is directly proportionally to the absorption coefficient of the chromophore, which changes based upon the wavelength of light used to excite the analyte. Thus, analyzing the amount of response observed can result in determination of the absorption coefficient, which is related to the amount of energy absorbed.

The pressure wave produced is proportional to energy per unit volume, J/cm<sup>3</sup>. When the spot size is held constant, the integral of pressure over depth yields the total absorbed energy as given in Equation 1.3

$$E_a = \int_0 p_0(z) dz \quad (1.3)$$

In Equation 1.3  $E_a$  is the total absorbed energy by the chromophore and  $p_0(z)$  is the initial pressure as a function of depth  $z$ . This integral gives a quantity expressed in terms of J/cm<sup>2</sup>. Thus, the amount of energy ( $E_a$ ) absorbed is directly related to the amount of incident light energy. Therefore we have a pressure wave that is proportional to the amount energy input into the system that is absorbed by the chromophore.

The detection of the acoustic waves generated by the aforementioned photonic excitation is inherently just as important as the mechanism by which the waves are generated. Modern photoacoustic methods use an array of sensors to detect these waves. Most typically used is some form of piezoelectric transducer. These transducers operate by utilizing a piezoelectric copolymer connected to two electrodes. One electrode is connected to the ground, while the other is attached directly to the copolymer in order to measure voltage changes across its surface. These copolymer films are typically constructed of polyvinylidene fluoride (PVDF). They can incorporate different elements to act as conducting agents, including but not limited to, silver, gold, or aluminum. When acoustic waves propagate through an acoustically favorable medium they impact the PVDF film on the surface of the transducer. This acoustic impact causes an electric field generated by the deformation of the PVDF (Viator *et al.*, 2002). These piezoelectric transducers are available commercially or can be manufactured cheaply with simple machining techniques (Viator *et al.*, 2002).

### 1.2.3 Current Research and Applications

In an age where technology is increasing at a seemingly exponential rate, it becomes imperative that ground breaking research in medical and commercial

applications take advantage of novel mechanisms for optical detection and imaging. Photoacoustics have been used to make three dimensional models of vasculature *in vivo* (Hoelen *et al.*, 1998; Kolkman *et al.*, 2003). Other techniques focus on detecting various chromophores present within a multitude of different media. The majority of these detection applications are based on the work done when photoacoustics resurfaced several decades ago. They use photoacoustics to detect different gases present in different media. However, The power of photoacoustic technology to determine the presence of significantly small particles makes its uses in these applications most compelling. One such technique employed by our group is the use of photoacoustics to indentify circulating metastatic melanoma cells (Weight *et al.*, 2006). Groundbreaking discoveries in the past several years have coupled photoacoustics with the attachment of nanoparticle tags. These tags can be used to enhance photoacoustic tomography (Yuan *et al.*, 2005) or to target cancer cells (Agarwal *et al.*, 2007). The field of photoacoustics encompasses many regimes of imaging and detection of various diseases, however, it has never been used to diagnose malaria infection. Thus, the work presented in this thesis is of unique consequence.

# Chapter 2

## Initial Design and Implementation

### 2.1 Specific Aims and Goals

The purpose of developing this system is to create a novel sensitive method that can screen large volumes of human cells for the presence of malaria. We propose to do so by studying the photoacoustic response of the malaria byproduct hemozoin at a multitude of visible wavelengths. We want to find the spectroscopic data associated with this unique optical absorber in order to determine which wavelengths will best be suited for a photoacoustic detection system. The subsequent data may be used to develop a method to optically determine the presence of hemozoin as an indicator of malarial infection.

We are going to acquire photoacoustic data from hemozoin at visible light wavelengths. The wavelengths we will use range from 410 to 650 nanometers. We are going to grow malaria infected erythrocytes (red blood cells) in a culture using standardized methods; we will then introduce human immunologically active white blood cells, or leukocytes. These leukocytes will then ingest the malaria parasites waste product known as hemozoin. These leukocytes will then be isolated and will be subjected to a range of light energy from multiple wavelengths using acrylamide wells to contain the sample. Once the sample is housed within the acrylamide well, an optical fiber coupled to a tunable laser system will deliver the light energy to the leukocytes. The photoacoustic responses will be collected by a transducer coupled to an oscilloscope.

### 2.2 Parasite Culturing

Initial parasite culturing followed tried and true culture methods as outlined by MR4 (Ljungstrom *et al.*, 2008). Wildtype parasites were obtained from active

cultures maintained by Dr. Beerntsen's lab members. They were cultured in T-25 flasks using media and blood as had been outlined by previous lab members and culture guidelines.

### **2.2.1 Blood**

O positive packed erythrocytes were obtained from Interstate Blood Bank (Interstate Blood Bank, Memphis TN). Upon arrival, the whole blood was allocated into several 50 milliliter conicals. Approximately 25 milliliters of packed erythrocytes were deposited into each conical. The conicals were centrifuged at 3000 RPM for 10 minutes. The buffy coat was carefully removed via pipette. RPMI 1640-11875 (Gibco, Carlsbad CA) was added to each conical until the total volume of each conical was 50 milliliters. The conicals were centrifuged again for 10 min at 3000 RPM. The supernatant was removed via pipette. This RPMI wash was repeated two more times. After the subsequent washes, RPMI was added until the suspension contained 50% RPMI and 50% packed erythrocytes.

### **2.2.2 Media**

Media was prepared using Albumax II (Gibco, Carlsbad CA) as prescribed by MR4(Ljungstrom *et al.*, 2008) and guidelines illustrated by other lab members. Two and a half grams of Albumax II were added to 500 milliliters of RPMI 1640-22400 (Gibco, Carlsbad CA) along with .025 g of Hypoxanthine (Sigma-Aldrich, St. Louis MO). A stir bar was added the solution and the media was agitated via a stir plate for 1 hour. The complete culture media supplemented with Albumax (CCMA) was then transferred into a biological safety hood. Prior to introducing the container to the sterile environment of the safety hood it was sanitized with 70% ethanol via a spray bottle. Once the CCMA was in the hood it was filtered with into a 500 milliliter vacuum driven filtration system (Fisher Scientific, Pittsburgh PA) to remove any bacteria or contaminants that may have allocated within the CCMA. The CCMA was then sterile and ready to be used for culturing purposes.



### **2.2.3 Culture Preparation**

A small volume of parasites was obtained from cultures either being actively carried by other lab members or retrieved from cryogenic storage. The cryogenic storage system was located on site. To initiate a culture, approximately .05 milliliters of erythrocytes exhibiting a 1% level of parasitic infection were deposited into a T-25 flask. To this flask 0.6 milliliters of the 50% whole blood solution was then added to the culture. Fourteen milliliters of CCMA was added to the culture and the culture was then aerated with a gaseous solution composed of 3% oxygen, 3% carbon dioxide, and 96% nitrogen gases. The flask was then stored in an incubator at 37°C. The cultures were checked approximately every 48 hours. In order to check the status of the cultures, microscopic analysis was used. The culture was removed from the incubator and the media was removed carefully with a pipette. One has to be very careful not to disturb the culture prior to this removal. The erythrocytes will have deposited on the floor of the flask allowing for easy removal of the media without accidentally removing part of the culture. After the media was removed, a small droplet of the infected erythrocytes was placed onto a standard microscope slide. A blood smear was then created by spreading the droplet with another slide. Once the slide has dried it was fixed by dipping it into a 50 milliliter conical containing pure methanol. The slide was submerged briefly and then allowed to dry. Once the slide had dried, several droplets of Giemsa stain (Sigma-Aldrich, St. Louis MO) were applied to the slide with a pipette. The complete area of the blood smear was covered with the stain. The stain was allowed to set for 10 minutes. After time had elapsed the slide was washed in running water and was then allowed to dry. After the slide was allowed to dry a drop of immersion oil was applied to the surface of the slide and the parasites were monitored at 100X magnification in order to determine their health and infection level.

### **2.2.4 Biology of White Blood Cells**

White blood cells, or leukocytes, are the body's first line of defense against invasion from foreign entities. The leukocytes defend the body against infecting

organisms and foreign entities in the tissues and in the bloodstream. Human blood contains approximately 10,000 leukocytes per microliter of blood. These leukocytes are differentiated into two categories, agranular and granular leukocytes.

The granular leukocytes form in the bone marrow and compose about 70% of all white blood cells. Granulocytes include three types of cells: neutrophils, eosinophils, and basophils. Neutrophils constitute the vast majority of granulocytes. Neutrophils are the chief phagocytic leukocyte and can engulf foreign bodies. This becomes of significant importance in our later research. They travel about the bloodstream and can surround and destroy bacteria and other foreign particles. The eosinophils, ordinarily about 2% of the granulocyte count, increase in number in the presence of allergic disorders and parasitic infestations. The basophils account for about 1% of the granulocytes. They release chemicals such as histamine and play a role in the inflammatory response to infection (Houghton Mifflin's The American Heritage Stedman's Medical Dictionary, 2005).

The agranular leukocytes include the monocytes and the lymphocytes. Monocytes are derived from the phagocytic cells that line many vascular and lymph channels. Monocytes ordinarily number 4% to 8% of the white cells (Houghton Mifflin's The American Heritage Stedman's Medical Dictionary, 2005). They move to areas of infection, where they are transformed into macrophages, large phagocytic cells that trap and destroy organisms not eradicated by the other leukocytes. In certain diseases of long duration, such as malaria, the monocytes act as the main instrument of defense (Houghton Mifflin's The American Heritage Stedman's Medical Dictionary, 2005). These agranular leukocytes can be isolated in the peripheral blood mononuclear layer using a Histopaque isolation. This is where our research initially focused upon.

### **2.2.5 Monocyte Isolation and Addition**

In order to examine the hemozoin contained within blood borne leukocytes, we had to develop a method for obtaining hemozoin laden leukocytes. Based on work performed by previous members of our lab (Weight *et al.*, 2006), a peripheral

blood mononuclear cell (PBMC) isolation was performed on blood samples obtained from volunteers. Upon creating a small culture within a T-25 flask, we added 0.1 milliliters of 50% leukocyte solution. These leukocytes were obtained by drawing fresh blood from live volunteers. This blood was then separated using a Histopaque 1077 isolation protocol. Three milliliters of Histopaque 1077 (Sigma-Aldrich, St. Louis MO) was placed within a 15 milliliter conical tube. Five milliliters of fresh whole human blood was then placed on top of the Histopaque without disturbing the surface of it. The conical was then centrifuged at 1800 RPM for 30 minutes with no brake. After centrifugation, the peripheral blood mononuclear cell (PBMC) layer could be seen floating on top of the Histopaque, the erythrocytes having now sunken below the Histopaque similar to the isolation seen in section 3.3.2. The PBMCs were carefully transferred to a clean conical with a pipette. The PBMCs were washed twice in 13 milliliters of RPMI 1640-11875 (Gibco, Carlsbad CA) for 10 min at 1600 RPM. The cell pellet was then suspended in 1 milliliter of RPMI 1640-11875. Then 0.1 milliliters of the PBMC suspension were added to the infected erythrocytes and allowed to incubate for 48-72 hours depending on the concentration of infected red blood cells. After incubation the mononuclear leukocytes (monocytes) should have ingested hemozoin from within the culture, thus gaining the malarial pigment. These Pigment Containing Monocytes (PCMs) were then separated from the infected cells using the same Histopaque isolation protocol that was used to initially separate the PBMCs from the whole blood. When applying this method of leukocyte addition and subsequent isolation we experienced very little success. A vast majority of the leukocytes would die in the culture. Furthermore, the monocytes seemed limited in their immunological activity. Upon microscopic inspection very little pigment could be seen ingested by the monocytes. This immunological inactivity was corrected by changing several of our culturing protocols. Switching to a media supplemented with human A positive serum as described in Section 3.3.2 was one of the things we changed. When we switched to a media supplemented with human serum an increase in the immunological activity of the monocytes was noticed via microscopic analysis. This overcame a major obstacle that we were facing during the initial

phases of culturing experiments. Another part of our protocol that we changed was the isolation of the monocytes. We began using a Histopaque isolation as prescribed earlier. This was later changed to a leukocyte enriched blood protocol as prescribed in Section 3.3.1. With the changes to our culturing media and blood collection process there was a marked increase in the number of immunologically active leukocytes observed within the culture. Through a serendipitous microscopic discovery, we learned that the granular leukocytes were ingesting hemozoin as well as the monocytes. Once we found a method of culturing the cells with immunologically active leukocytes we merely had to isolate them. This led to an alteration of our final isolation protocol. We switched to a different Histopaque gradient that allowed isolation of the monocytes as well as the granulocytes. This protocol is outlined in Section 3.3.2.

## **2.3 Initial Photoacoustic Tests**

### **2.3.1 Acrylamide Well Preparation**

Based upon previous work, sample wells were created using an acrylamide gel. The well housing was created with a circular piece of PVC pipe. The pipe had a diameter of 38 mm and a depth of 9.4 mm. The piece of PVC had commercial plastic wrap stretched over the underside which was held in place by a rubber band. An acrylic rod was suspended over the piece of PVC to create the well when the subsequent acrylamide solution was added to the well housing as seen in Figure 2.1. The acrylamide solution was created by adding 20 grams of acrylamide (Sigma-Aldrich, St. Louis MO) with .7 grams of bis-acrylamide (Sigma-Aldrich, St. Louis MO) per 100 milliliters of deionized water. Ten milliliters of this acrylamide solution was combined with 0.06 grams of ammonium persulfate (Sigma-Aldrich, St. Louis MO) and 1 milliliter of 20% Intralipid (Fresenius Kabi, Hamburg Germany) solution in a small beaker and a stirring rod was added. After the solution was allowed to mix thoroughly 60  $\mu\text{L}$  of TEMED (Sigma-Aldrich, St. Louis MO) was added and the solution was immediately poured into the well housing as shown in

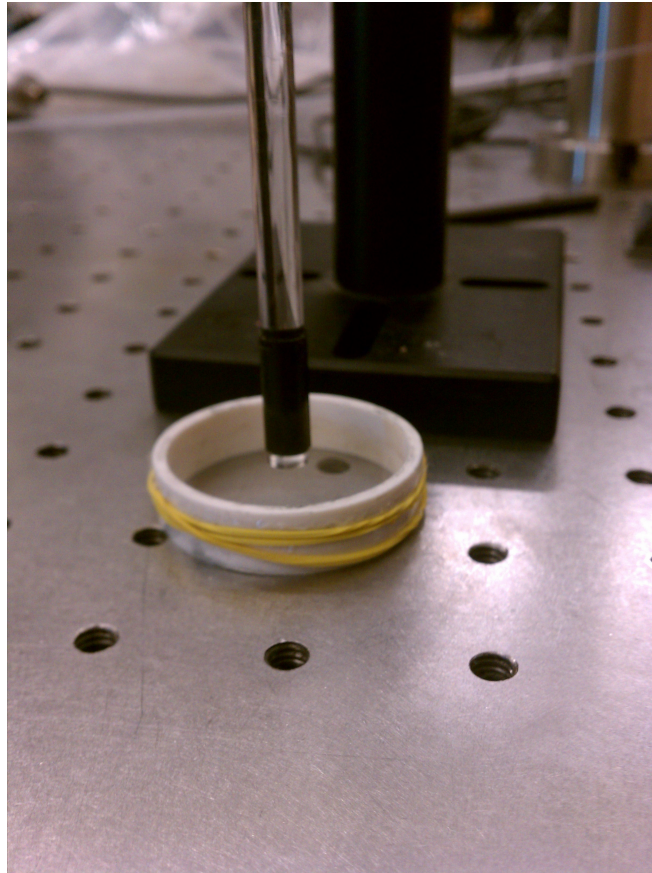


Figure 2.1: Image of the Well Housing

Figure 2.2. The well created had a total depth of 2 mm and a diameter of 6.4 mm, creating a well volume of 60  $\mu\text{L}$ . The final well can be observed in Figure 2.3.

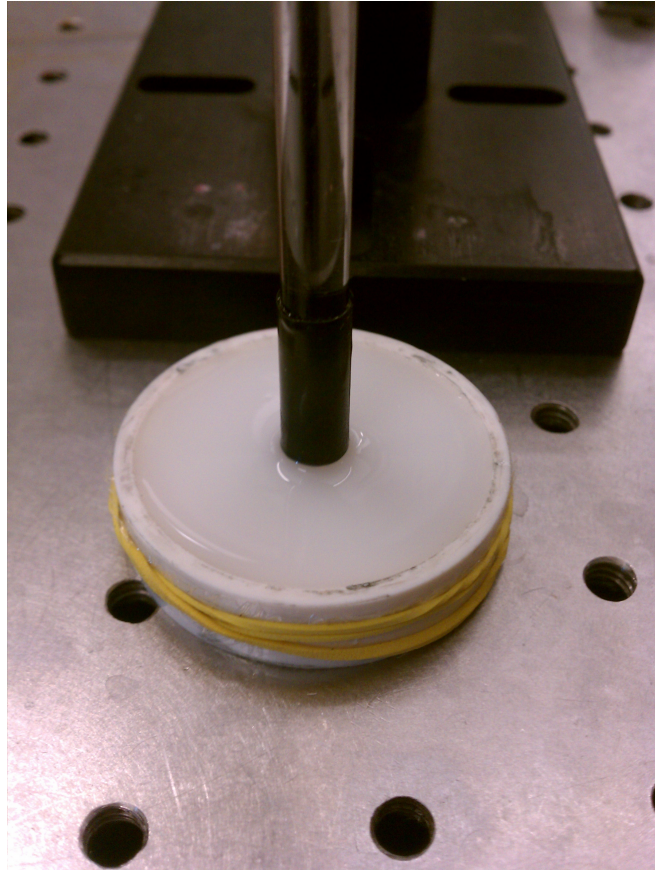


Figure 2.2: Acrylamide Solution After Being Poured Into the Well Housing



Figure 2.3: Image of the Well After it Has Solidified

### 2.3.2 Piezoelectric Transducer Manufacturing

Piezoelectric transducers can be manufactured in a number of inexpensive effective ways as shown by previous work (Viator *et al.*, 2002). You will need a piezoelectric copolymer connected to two electrodes. One electrode is connected to the ground, while the other is attached directly to the copolymer in order to measure voltage changes across its surface. These copolymer films are typically constructed of polyvinylidene fluoride (PVDF). They can incorporate different elements to act as conducting agents, including but not limited to, silver, gold, or aluminum. When acoustic waves propagate through an acoustically favorable medium they impact the PVDF film on the surface of the transducer. This acoustic impact causes an electric field generated by the deformation of the PVDF (Viator *et al.*, 2002). Our initial transducer was constructed using gold plated PVDF. A copper core was inserted into an acrylic cylinder. A small strip of PVDF was then glued to the top of the acrylic cylinder with the gold plated side of the PVDF facing outward. The strip was then folded downward along the edge of the cylinder and attached to a conductive housing. The copper core was attached to the ground of a coaxial cable and the housing conducted the voltage changes that occur due to the PVDF deformations caused by the acoustic pressure waves.

### 2.3.3 Acrylamide Well Tests

An acrylamide well was prepared as described earlier. The well was placed on top of a piezoelectric transducer. Acoustic gel was used to couple the well to the transducer in order to ensure propagation of the acoustic pressure waves. A 60  $\mu\text{L}$  sample of PCLs obtained as described in Section 3.3.2 was placed within the well using a micropipette. The hemozoin laden leukocytes were excited using a tunable laser system coupled into an optical fiber. The fiber was placed 2 mm above the sample and a single pulse of laser light was used to excite the sample at a given wavelength. A Q-switched Nd:YAG Vibrant 355 II laser (OPOTEK Inc., Carlsbad CA) with a pulse duration of 5 ns was used to excite the PCLs, the wavelengths ranged from 420 nm to 670 nm, and the laser energy ranged from approximately





Figure 2.4: Top View of the Piezoelectric Transducer



Figure 2.5: Side view of the piezoelectric transducer

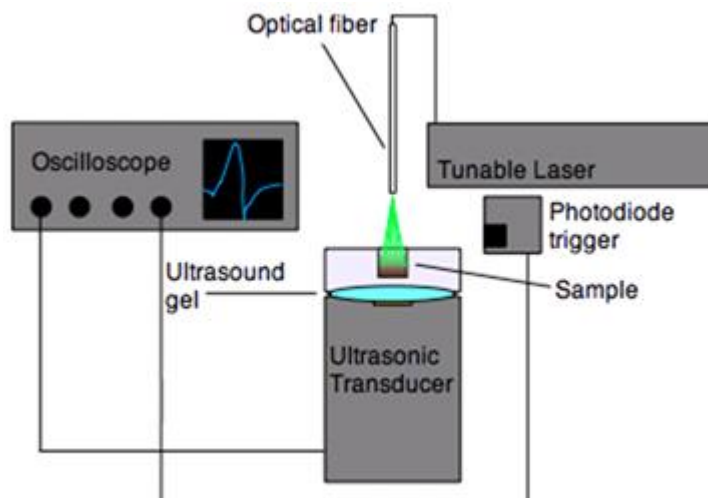


Figure 2.6: Model of Original Photoacoustic Setup

1-4 mJ. A glass slide was used as beam splitter to measure the energy from the laser. The energy was measured with an energy sensor model number J-25mB-HE (Coherent Inc., Santa Clara CA) connected to an energy meter model Fieldmax TOP (Coherent Inc., Santa Clara CA). The signals were processed by being fed into a Tektronix TDS 2024B oscilloscope (Tektronix Inc., Beaverton OR) where the photoacoustic waveforms were analyzed and then saved. An illustration of the photoacoustic setup can be seen in Figure 2.6. A  $60 \mu\text{L}$  sample was placed into the system and a single pulse of laser light was fired into the sample. The wavelengths started at 670 nm. After excitation the energy was recorded and the signal was saved via the oscilloscope. The sample was rinsed out of the well and a new sample was placed into the well. The wavelength was decremented by 10 nanometers and the process was repeated until the wavelength reached 420 nm. The photoacoustic pressure responses were normalized by their energies and the subsequent data was graphed. This can be seen in Figure 2.7

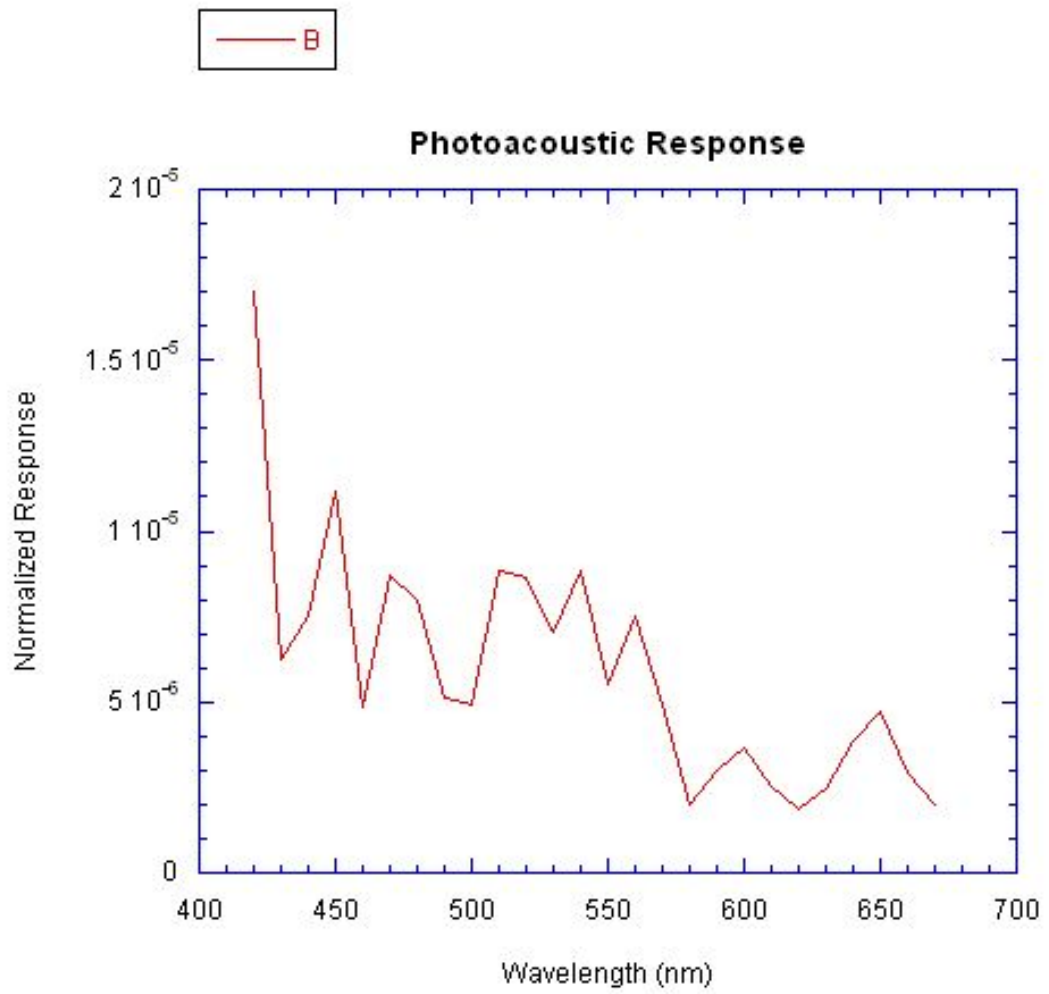


Figure 2.7: Data Obtained From Original Photoacoustic Setup

As can be seen, the resultant data was highly erratic. This is caused by the inability to take multiple samples at each wavelength. Due to the size of the wells used, the sample ran out very quickly. Also, since the sample is a biologically cultured sample it can take weeks to cultivate. A system that uses a smaller sample size was needed in order to effectively measure the photoacoustic responses of the pigment laden leukocytes. Furthermore, due to the placement and close proximity of the optical fiber, degradation of the PVDF element on the piezoelectric transducer was noted. This caused inaccurate measurement of the photoacoustic responses.

### 2.3.4 Initial Flow system Tests

Other members of our lab have been working on a two phase microfluidic photoacoustic detection system to test for malignant metastatic melanoma cells (Weight *et al.*, 2009; O'Brien *et al.*, 2010; O'Brien *et al.*, 2011). Due to the design of the system, large quantities of cells can be scanned very quickly in a microfluidic environment. The sample size is significantly smaller, 2-3  $\mu$ liters. Furthermore, the optical fiber is placed orthogonally to the transducer. With a much smaller sample size, we can take multiple measurements without having to significantly dilute the sample. Also, the orthogonal placement of the optical fiber that is coupled to the laser significantly reduced the risk of damaging the transducer during our photoacoustic excitations of the sample. Using a self assembled transducer along with the two phase flow system we recorded an array of photoacoustic spectral analysis. The first tests were recorded using two phases, one composed of air and the other composed of water. We measured the energy with the same equipment as in previous experiments. The laser was split using a glass slide prior to being coupled and directed towards an energy sensor. A 2  $\mu$ liter slug containing our sample was directed in front of our detection area. A single pulse of laser energy was used to excite the slug and the photoacoustic response was recorded on the oscilloscope as described previously. This was repeated for wavelengths ranging from 410-650 nanometers. Five samples were taken at each wavelength. The energy reading measured pre-coupling were fairly constant. This should not have been the case.

There could have been a number of reasons that this happened. It could have been caused by a bad sensor, or even a poor connection with the energy meter. Therefore, when we normalized our data with the energy readings, the data did not follow the trends we expected and was highly erratic. This can be seen in Figure 2.8

In order to correct for this, we changed how we measured the energy. Instead of measuring the energy prior to fiber coupling, we measured the energy post sample. We aligned the energy sensor parallel to the optical fiber so that after the light had passed through the sample it became incident upon the sensor. This greatly improved our results as can be seen in Figure 2.9.

While this data shows marked improvement and correlates more closely with similar photoacoustic response experiments involving hemozoin (Hempelmann & Marques, 1994; Balasubramanian *et al.*, 1984), it still was not within the confines of sound repeatable data. The next improvement made to the system was the introduction of a commercially manufactured transducer. We replaced our self assembled PVDF transducer with a 0.5 inch focused polyvinylidene fluoride transducer PI20-2-R1.50IN (Olympus, Waltham MA). Furthermore, due to inherent pressure variations within the two phase flow system, the bubble size was not consistent throughout the experiments. The addition of a surfactant to the PCLs was the next step we took in order to get more accurate data, with a consistent bubble size.

### **2.3.5 Tween 80 Surfactant Experiment**

We added 2% per volume of Tween 80 to a sample of freshly obtained human leukocytes. The sample was allowed to sit for 10 minutes, and the solution was observed under a microscope. The cells appeared to be unaffected by the surfactant. Therefore, after culturing another sample of PCLs we added 2% per volume of Tween 80 to the sample and proceeded to setup up our two phase flow system. Upon beginning the experiment it became clear that we were not getting photoacoustic responses from the sample. Visual inspection of the sample showed that prolonged exposure to the surfactant had an effect on it. The leukocytes had aggregated into a

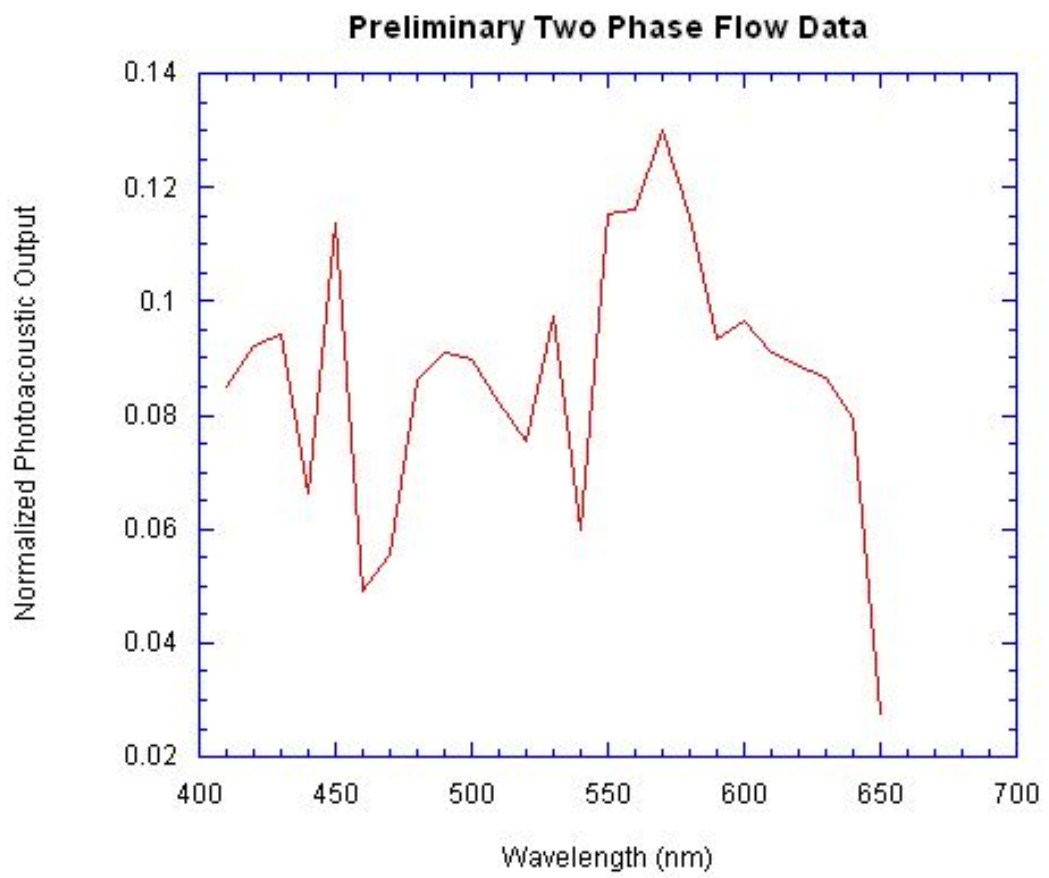


Figure 2.8: Preliminary Two Phase Flow Data

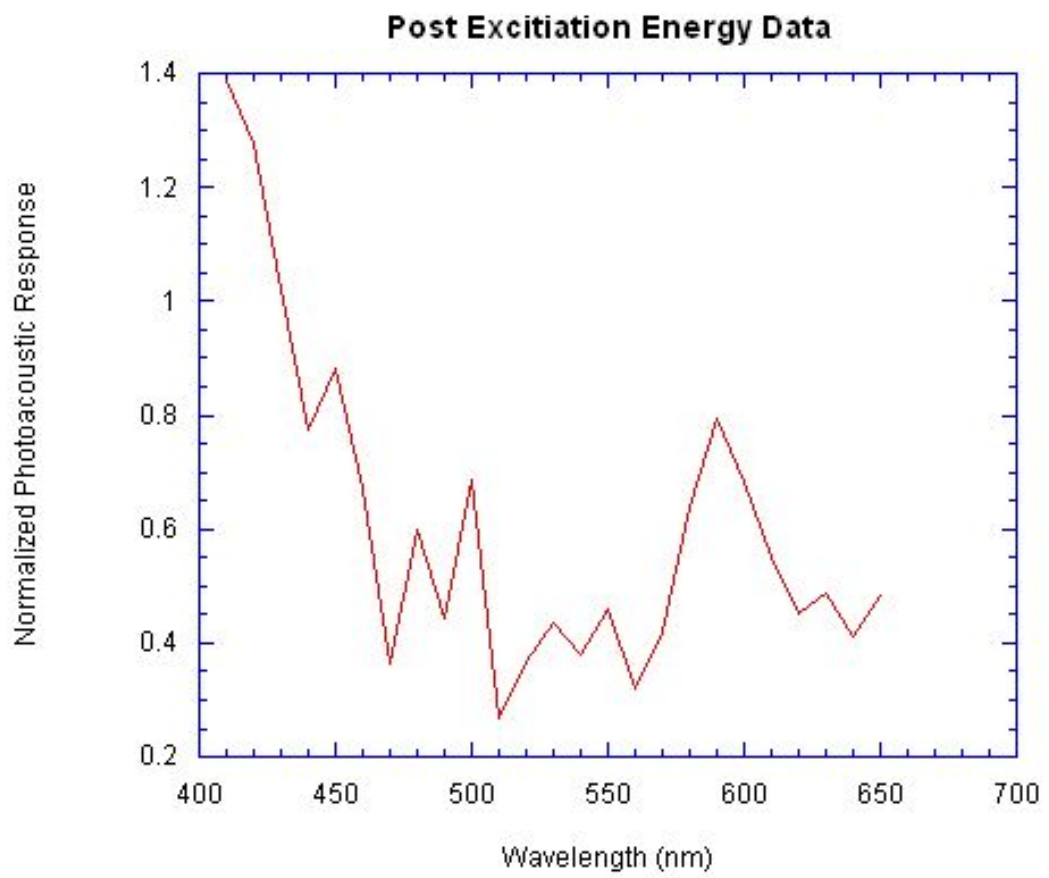


Figure 2.9: Post Excitation Resultant Data



large mass of hemozoin laden material. We decided that rather than discarding the sample we would mechanically separate it and perform static photoacoustic tests on it. The sample was mechanically separated into 4 discrete samples of similar size. Each sample was placed on a 1 mm thick scattering pad that was placed on top of a 1 mm thick black absorption pad that separated the sample from the transducer. A 0.5 inch focused polyvinylidene fluoride transducer PI20-2-R1.50IN (Olympus, Waltham, MA, 02453, USA) was used to detect the photoacoustic response of the sample. The sample was irradiated via an optical fiber from above at a distance of 1 mm from the sample. A frequency-tripled Q-switched Nd:YAG Vibrant 355 II laser system (Opotek Inc., Carlsbad CA) was used to excite the hemozoin samples. The pulse duration was 5ns, the wavelength ranged from 410 nm to 650 nm, and the laser energy ranged from 2-4 mJ. The signals were processed using a RITEC Broadband Receiver Model BR-640A (Ritec, Rochester NY) where the signal was filtered and amplified to 32 dB, before being fed into a Tektronix TDS 2024B oscilloscope (Tektronix Inc., Beaverton OR) where the Photoacoustic waveforms were analyzed and then saved. A single shot at each wavelength was taken to prevent photo bleaching, starting at 650 nm, and moving down to 410 nm in decrements of 10 nm. After the spectrum was complete, the evaluated section of hemozoin was removed, and a new section was placed on the transducer setup for evaluation. This was done with all four sections of the hemozoin sample. The energy of each laser pulse was measured prior to coupling in the optical fiber by using a beam splitter and an energy sensor as described in earlier methods. These energy measurements were used to normalize the data.

The acrylamide solution was prepared using 20g acrylamide (Sigma-Aldrich, St. Louis MO) combined with .7g Bisacrylamide (Sigma-Aldrich, St. Louis MO) per 100 mL of deionized water. To make a black absorption pad, 5 mg of Chlorazol black (Sigma-Aldrich, St. Louis MO) was added to 5 mL of the acrylamide solution, next 20 mg of ammonium persulfate (Sigma-Aldrich, St. Louis MO) was added. The solution was allowed to mix thoroughly before finally adding 20  $\mu$ l of Tetramethylethylenediamine (TEMED) (Fisher Scientific, Pittsburgh PA). The

solution was then quickly poured into a 1 mm deep square mold to create a thin pad.

The Scattering pad was made using 5 mL of the acrylamide solution, 75  $\mu$ l of 20% Intralipid (Fresenius Kabi, Hamburg Germany) and 20 mg of ammonium persulfate. The solution was allowed to mix thoroughly before finally adding 20  $\mu$ l of TEMED (Fisher Scientific, Pittsburgh PA) . After adding the TEMED, The solution was then rapidly poured into a 1 mm deep square mold to create a thin pad.

The data acquired followed the other spectral data that we had acquired, as well as other research into hemozoin and heme based proteins (Bohle *et al.*, 1994; Hempelmann & Marques, 1994; Faber *et al.*, 2003). Each photoacoustic response was analyzed to determine a peak to peak output magnitude. These magnitudes were normalized using the energy measurements recorded during the experiment. The data showed output that coincided with our knowledge of the hemozoin spectrum. The data was somewhat inconsistent though. I felt that the standard deviation was too large and wanted a more repeatable system for analysis. The data was averaged and a standard deviation was calculated using Kaleidagraph. The graphed output can be seen in Figure 2.10.

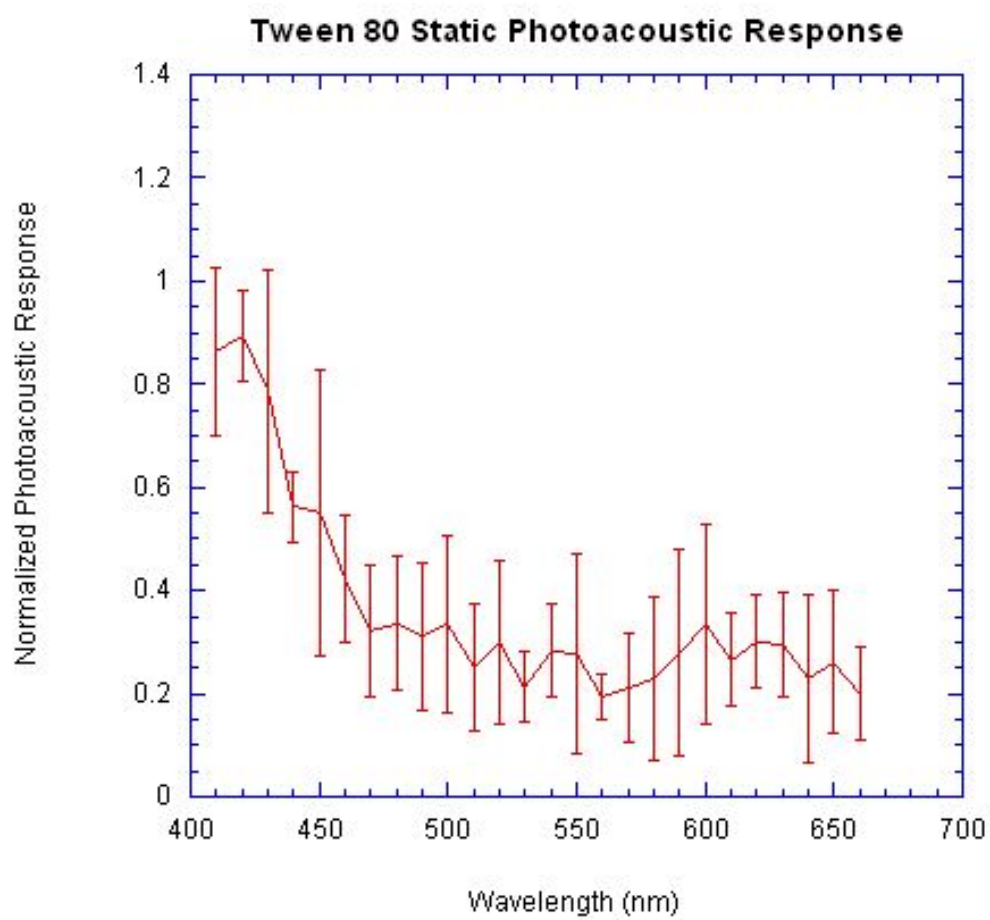


Figure 2.10: Tween 80 Static Photoacoustic Response

Finally, we integrated the use of our system reported in Sections 3.3.4 and 3.3.5. We were now using a commercial grade transducer, and measuring our energy post excitation. The slug size was still slightly inconsistent, but approximately  $2 \mu\text{l}$ . Since the addition of the surfactant had caused the cells to aggregate we had no other means of lubricating the microfluidic two phase system. However, we tried to gather spectral data using the two phase flow system. The data was gathered as explained previously, using single pulses at each wavelength, per each slug. The resultant data varied widely as can be seen in Figure 2.11. This led to the laminar flow used to acquire the spectral responses as described in Section 3.3.5. While the two phase flow system proved poor at the diagramming of photoacoustic responses, it did detect the cells, and allow for isolation of each slug.

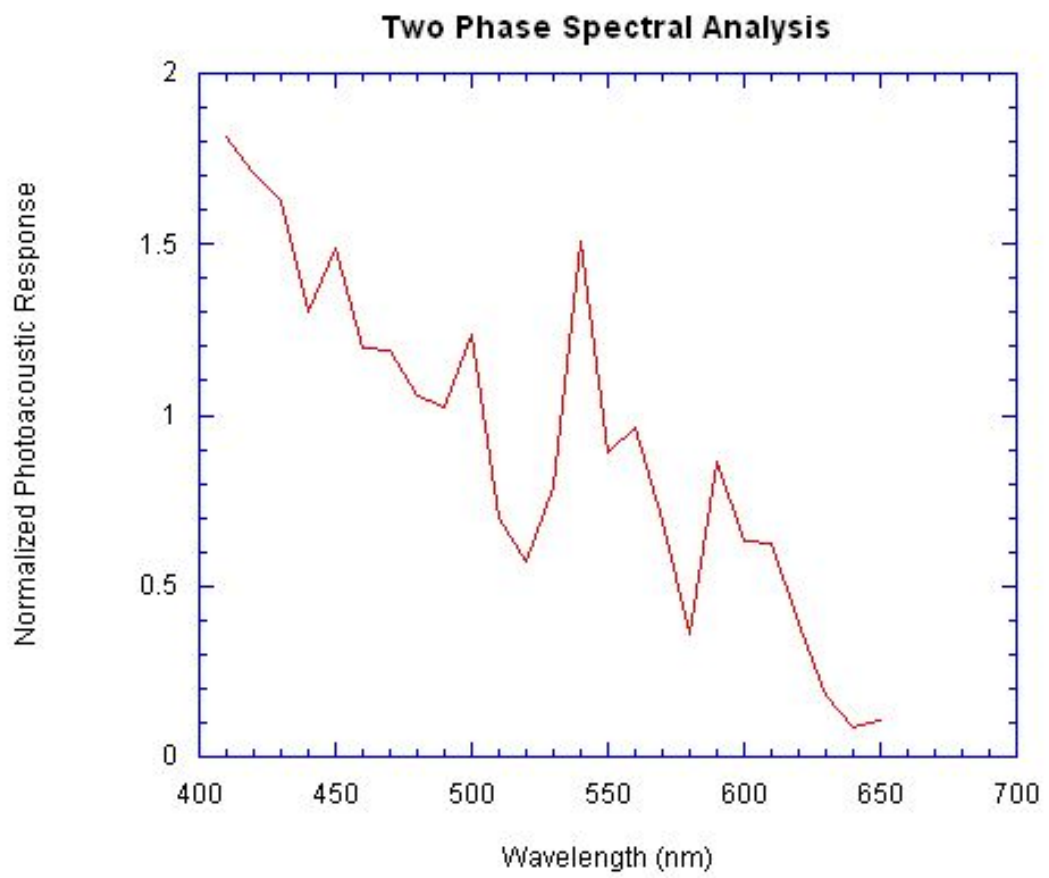


Figure 2.11: Final Two Phase Flow Photoacoustic Response

# Chapter 3

## Final System Design

### 3.1 Abstract

Malaria is a blood borne infection affecting hundreds of millions of people worldwide. The parasites that cause this disease reproduce within the red blood cells, eventually causing their death and lysis. This process releases the parasites into the blood, continuing the cycle of infection. Usually, malaria is diagnosed only after a patient presents symptoms, including high fever, nausea, and, in advanced cases, coma and death. While reproducing within the bloodstream of a host, malaria parasites convert hemoglobin into an insoluble crystal, known as hemozoin. These crystals, approximately several hundred nanometers in size, are contained within red blood cells and white blood cells that ingest free hemozoin in the blood. Thus, infected red blood cells and white blood cells contain a unique optical absorber that can be detected in blood samples using photoacoustic detection methods. Our group separated the white blood cells from malaria infected blood and tested it *in vitro* using a photoacoustic set up with a tunable laser system consisting of an optical parametric oscillator pumped by an Nd:YAG laser with pulse duration of 5 ns. These cells were tested at multiple wavelengths, and results imply the potential to assay simple blood draws from healthy and infected patients for the presence of hemozoin, thus providing a novel method for the indication of malaria infection.

### 3.2 Introduction

Nearly 3.3 billion human beings live in regions of the world where malaria is endemic, meaning that both the parasites that cause the disease, as well as the vectors that bear the disease are present. There are approximately 250 million cases of malaria contracted annually resulting in the loss of approximately 1 million lives,

most of which belong to sub-Saharan African youth (WHO, 2011). The malaria parasite is borne by the mosquito of the genus *Anopheles*. Nearly 40 different species of the aforementioned genus can transmit the disease. These species inhabit the majority of human populated regions. While the disease is not always present in the same areas as the vector, there is a chance that the parasite could spread into other regions than it currently inhabits, i.e. the United States (Zucker, 1996).

Malaria is caused by infection from a blood borne eukaryotic protist of the genus *Plasmodium*. There are three main species of the plasmodium parasite that infect humans: *P. vivax*, *P. ovale*, and *P. falciparum*. *P. falciparum* is the most damaging to humans. Its symptoms include, but are not limited to, high fever, chills, nausea, sweats, muscle aches, tiredness, anemia, jaundice and, in advanced cases, kidney failure, seizures, coma, and death (CDC, 2011). The symptoms caused by *P. vivax* and *P. ovale* are similar, but often much less severe. *P. falciparum* is the most prevalent species of plasmodium accounting for a majority of all malarial infections (WHO, 2011). *P. falciparum* has two distinct phases of its life cycle: the invertebrate stage and the vertebrate stage, the latter of which is most pertinent to our research. The vertebrate stage of the parasites life cycle begins with the bite of a female *Anopheles* mosquito. When the bite is initiated, the mosquito injects its saliva into the host organism in order to numb the tissue so that it may feed undisturbed. However, a mosquito that is infected with *P. falciparum* will unknowingly inject sporozoites carried within the saliva. These sporozoites, which are about 1  $\mu\text{m}$  in diameter and 10-15  $\mu\text{m}$  in length (Roberts & Janovy, 2008), travel through the blood stream where they are deposited in the liver. In the liver, they invade the hepatic cells. During the next 10-14 days the sporozoites differentiate and undergo schizogony, a form of asexual reproduction in which multiple mitoses take place, followed by simultaneous cytokinesis, resulting in many daughter cells at once (Roberts & Janovy, 2008). These daughter cells are called merozoites. Upon lysis of the hepatic cells thousands of merozoites are released into the blood stream where they begin to invade the host erythrocytes (red blood cells). This invasion of the host erythrocytes marks the beginning of *P. falciparum*'s

asexual erythrocytic reproductive cycle. Upon entry into the host erythrocytes, the merozoites differentiate into trophozoites. Initially, host cytoplasm ingested by the trophozoite forms a large food vacuole, which gives the parasite a ring-like appearance where-in the nucleus lies along the outer circumference of the ring when examined with light microscopy. As the parasite grows in size, the appearance of the food vacuole becomes less prevalent. However, hemozoin crystals begin to aggregate and become visible in the food vacuole. Hemozoin is the byproduct of *P. falciparum*'s consumption of the hosts hemoglobin within the erythrocyte. When the trophozoite is mature it undergoes schizogony, thus rapidly developing into a schizont. This schizont houses 8-20 merozoites. Once the merozoites are mature, the erythrocyte ruptures, thus releasing the merozoites, as well as metabolic wastes, including hemozoin. The merozoites are then free to invade new erythrocytes and the process repeats itself approximately every 48 hours as diagramed in the introduction.

During the trophozoite stage of the *Plasmodium* life cycle, parts of the erythrocyte are consumed by the parasite. Nearly 90% of the protein contained within the erythrocyte is contributed by the hemoglobin (Jani *et al.*, 2008). During the metabolic breakdown of hemoglobin, large quantities of heme are released. This heme is toxic to biological cells and the parasite utilizes a novel mechanism where it rapidly converts heme into a crystalline material known as hemozoin (Jani *et al.*, 2008). Hemozoin is an insoluble crystalline polymer which has unique optical absorbance properties. This optical absorber can be found free floating in the blood stream of subjects who exhibit malarial infection. This polymer can also be found within erythrocytes where *P. falciparum* is incubating, as well as within host leukocytes (white blood cells) (Clark & Tomlinson, 1949; Nguyen *et al.*, 1995).

By examining the biology of the parasite it becomes apparent that the hemozoin created by the infection is prevalent throughout the hosts system (Clark & Tomlinson, 1949; Nguyen *et al.*, 1995). By adding light energy to the hemozoin present in the system we can create acoustic images of the hemozoin. When rapid pulses of light are applied to an analyte, the energy can be absorbed and briefly stored. This energy causes thermoelastic expansion which in turn produces



detectable sound waves due to pressure variations created in the surrounding medium (Viator *et al.*, 2002). The photoacoustic effect is a conversion from light energy to acoustic waves, due to this absorption and localized thermal excitation. The intensity of the sound waves is proportional to the intensity of the light energy input to the system. By using a high intensity light source, a greater intensity sound can be generated. Hemozoin is an optical absorber, and is only present in patients who exhibit malarial infection. Therefore, analyzing the hemozoin captured within the leukocytes with photoacoustic methods, we can determine malarial infection based on the presence of the hemozoin crystals. While photoacoustic spectroscopy of hemozoin has been explored previously (Balasubramanian *et al.*, 1984), it has never been used to diagnose infection.

### **3.3 Materials and Methods**

#### **3.3.1 Leukocyte Laden Blood**

Fresh whole human blood was drawn from a volunteer. The same volunteer was used throughout the duration of our experiments. Using the same person for subsequent blood acquisitions eliminates variations in blood characteristics that differ from person to person. The blood samples were collected in 10.8 mg EDTA coated 5 ml vacutainers (BD, Franklin Lakes NJ). Approximately 20 ml of blood was obtained for use in cultivation. The blood was collected from the tubes and transferred into 2 separate 15 ml conicals. The conicals were centrifuged at 3500 RPM for 10 minutes. The blood plasma was then removed using a pipette, while carefully leaving the buffy coat intact. The buffy coat is the layer of leukocytes and platelets that remains after centrifugation. RPMI 1640-11875 (Gibco, Carlsbad CA) was added to each conical until the total volume within the conical was 13 ml. The solution was gently aerated using a pipette and then centrifuged at 3500 RPM for 10 min. The wash was repeated two more times, each time carefully ensuring the buffy coat stay intact. After the third wash, the buffy coat, along with approximately 1 ml of blood, was carefully removed from the sample via pipette. This sample was

then added to a clean 15 ml conical and suspended with 50% RPMI 1640-11875. This erythrocyte and leukocyte solution is referred to as leukocyte enriched blood in further methods.

### 3.3.2 Pigment Containing Leukocytes

In order to examine the hemozoin contained within blood borne leukocytes, we had to develop a method for obtaining hemozoin laden leukocytes *in vitro*. Wild type *Plasmodium falciparum* parasites were obtained from Malaria Research and Reference Reagent Resource Center ([www.mr4.org](http://www.mr4.org)). *P. falciparum* infected erythrocytes were cultured as outlined by the Methods of Malaria Research (Ljungstrom *et al.*, 2008). They were cultured using RPMI 1640-22400 (Gibco, Carlsbad CA) supplemented with 10% A positive human serum (Interstate Blood Bank, Memphis TN) and .05g/L of Hypoxanthine (Sigma-Aldrich, St. Louis MO). The serum supplemented media was chosen as we had experienced difficulty sustaining immunologically active white blood cells in media supplemented with Albumax (Gibco, Carlsbad CA 92008), as prescribed for culture use by MR4 (Ljungstrom *et al.*, 2008). We added .6 ml of our leukocyte enriched blood solution to a T-25 flask containing  $\sim$ .05 ml of erythrocytes at a 1% parasitemia level. The culture was then allowed to incubate for  $\sim$ 48 hours. The culture was collected via pipette and transferred to a 15 ml conical. The conical was centrifuged for 10 min at 3500 RPM. The media was removed via pipette until 5 ml of culture and media remained. The remaining culture with media was then gently aerated with a pipette. After incubation the leukocytes have ingested hemozoin created by the parasites. Now we have a vehicle for transporting and examining the malaria pigment. We call these cells Pigment Containing Leukocytes (PCLs). This culture was separated using a Histopaque 1119 (Sigma-Aldrich, St. Louis MO) isolation protocol. Five ml of Histopaque 1119 was placed within a 15 ml conical tube. Five ml of cultured sample was then placed on top of the Histopaque without disturbing the surface of the Histopaque. The conical was centrifuged at 1800 rpm for 30 minutes with no brake. After centrifugation, the PCLs could be seen floating on

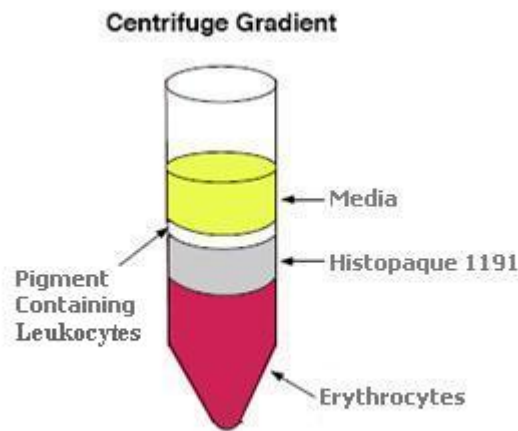


Figure 3.1: PCL Histopaque 1191 Isolation

top of the Histopaque, the erythrocytes having now sunken below the Histopaque as outlined in Figure 3.1. The PCLs were carefully transferred to a clean 15 ml conical with a pipette. Approximately 2 milliliters of Promega cell lysis solution (Promega Corporation, Madison WI) was added to the PCLs. The solution is allowed to sit for 10 minutes while agitating the solution once after 5 minutes. The cell lysis solution is used to ensure that any erythrocytes that may have remained in the solution have been eliminated. The solution was then centrifuged for 8 min at 1400 RPM. The PCLs were washed twice in 13 ml of 1X PBS (Fisher Scientific, Pittsburgh PA) for 10 minutes at 1600 RPM. The cell pellet was then suspended in 6 ml of 1X PBS. These PCLs were analyzed via light microscopy to ensure they had indeed gained the malaria pigment and that other optical absorbers had been eliminated.

### 3.3.3 Flow Chamber Design

A single cell can be considered an optical point source and will therefore emit photoacoustic waves radially. Therefore, a detection chamber in which the point of optical excitation is parallel to the transducer creates a system where the transducer

is not subject to direct exposure to the laser energy. This creates a situation where we can still monitor acoustic pressure waves without risk of damaging the transducer. The flow chamber, shown in Figure 3.3, was held together with an acrylic ring that had three holes drilled at 90° from each other. Masterflex (Vernon Hills IL) tubing was fed through the holes and a wire with the same outer diameter as the tubing inner diameter was suspended through the two opposing holes while a second wire was fed through the third hole to prevent acrylamide from entering the tubing hole. Once the acrylic ring was prepared, Parafilm was stretched across the bottom of the ring and clear acrylamide was poured into the ring, gelling around the tubing and wire. The acrylamide solution was prepared using 20g acrylamide (Sigma-Aldrich, St. Louis MO) combined with .7g Bisacrylamide (Sigma-Aldrich, St. Louis MO) per 100 mL of deionized water. The acrylamide for the chamber was made from 10 mL of the aforementioned acrylamide solution, 0.04g of ammonium persulfate (Sigma-Aldrich, St. Louis MO) and 20  $\mu$ L of Tetramethylethylenediamine (TEMED) (Fisher Scientific, Pittsburgh PA) were added to polymerize the solution into a gel. After adding the TEMED, the mixture was poured immediately to avoid premature gelling. After gelling, the wires were removed and the third tubing was used to hold the optical fiber in place, aiming at the flow path. The flow chamber was then ready to be used in the system.

### 3.3.4 Two Phase Photoacoustic Detection and Isolation

Photoacoustic flowmetry is similar to classic flow cytometry; a sample of interest is directed past a detector to identify if a certain analyte is present. Unlike flow cytometry, millions of cells can flow past the detector at a time due to the photoacoustic transparency of white blood cells (Weight *et al.*, 2009; O'Brien *et al.*, 2010; O'Brien *et al.*, 2011), allowing large volumes to be scanned very quickly for the presence of PCLs.

The system reported is shown in Figures 3.2 and 3.3 and is different from most other microfluidic systems due to its size and shape. The system was composed of cylindrical silicone tubing, which behaves slightly differently than square edge

systems. Although a classic microfluidic system utilizes channel dimensions lower than 100  $\mu\text{m}$  and flow rates less than 1  $\mu\text{L/s}$ , our system used an inner tubing diameter of 1.6 mm and the flow rates used were 100  $\mu\text{L/min}$ . It has been observed that two slugs of immiscible fluids can be created when both phases are input to a T-junction under microfluidic conditions (Garstecki *et al.*, 2006; Gupta & Kumar, 2010; Thorsen *et al.*, 2001; Tice *et al.*, 2004). For a given set of flow rates, the sizes of the slugs remain constant and the total flow rate of the mixture is the sum of the flow rates. A given slug flows past the photoacoustic detector and it is excited with a single laser pulse. The photoacoustic pressure wave created is stored onto a USB drive via the Tektronix oscilloscope. Since the flow-rate of the fluid mixture is known, the slugs can be tracked individually and separated from each other.

A 0.5 inch focused polyvinylidene fluoride transducer PI20-2-R1.50IN (Olympus, Waltham MA) detected the photoacoustic response of hemozoin contained within the PCLs. The transducer was sandwiched between a Polydimethylsiloxane (PDMS) base, and a 1.5 mm thick ring that covered the top of the brass housing, yet still revealing the PVDF element to prevent acoustic reflections. The transducer was fitted into a PVC holder that helps align the transducer, the PDMS components, and finally the flow chamber, as shown in Figures 3.2 and 3.3.

A Q-switched Nd:YAG Vibrant 355 II laser (OPOTEK Inc., Carlsbad CA) was fired at a right angle to the transducer, aligned on the side of the flow chamber. The pulse duration was 5 ns, the wavelength ranged from 410 nm to 650 nm, and the laser energy ranged from approximately 1-3.5 mJ. The signals were processed using a RITEC Broadband Receiver Model BR-640A (Ritec, Rochester NY) where the signal was filtered and amplified to 32 dB, before being fed into a Tektronix TDS 2024B oscilloscope (Tektronix Inc., Beaverton OR) where the Photoacoustic waveforms were analyzed and then saved.

The flow chamber was connected to two syringe pumps Braintree model BS 8000 (Braintree Scientific Inc, Braintree MA); one syringe contained the cell sample and the other contained air. The air was pumped at 0.1 mL/min and the sample was pumped at 0.1 mL/min. The syringe pump that housed the cells was set vertically

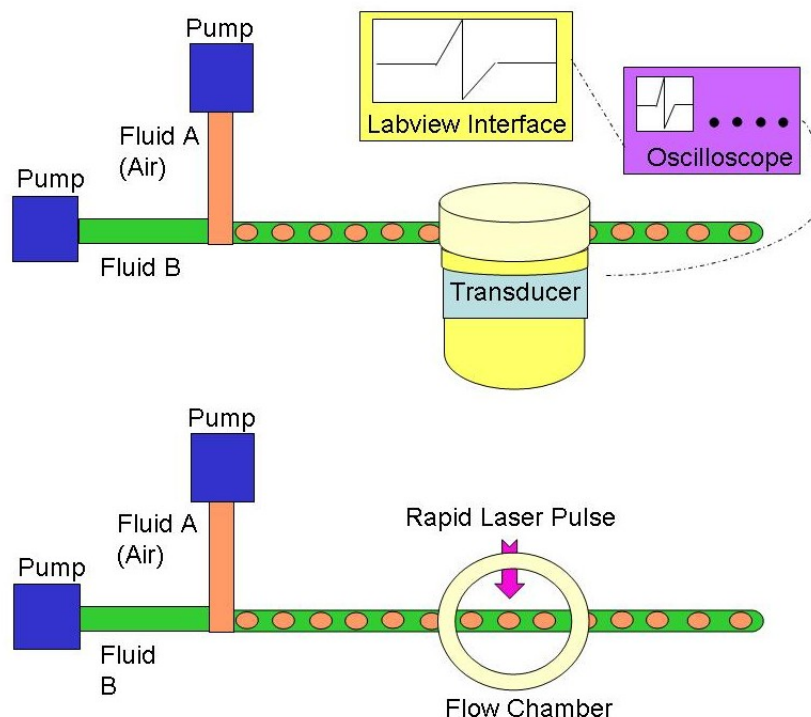


Figure 3.2: Schematic of Photoacoustic Flow System from Side and Top Views

to ensure the cells flowed unabated to the end of the syringe.

### 3.3.5 Single Phase Photoacoustic Spectral Analysis

The PCLs were suspended in 6 ml of 1X PBS as previously described. This solution was then inserted into a 10 ml syringe to be used in the photoacoustic flow system. The system was setup similarly to the two-phase flow system, except that only a single pump was utilized to create constant laminar flow at a rate of  $100 \mu\text{L}/\text{min}$ . This flow was subjected to single pulses of 5 ns duration from the Vibrant II laser system. This was done for wavelengths ranging from 650-410 nm stepping in 10 nm decrements. The energy was measured post sample with an energy sensor model number J-25mB-HE (Coherent Inc., Santa Clara CA) connected to an energy meter model Fieldmax TOP (Coherent Inc., Santa Clara CA). The data was collected after each laser excitation via the Tektronix oscilloscope. This was repeated 5 times for

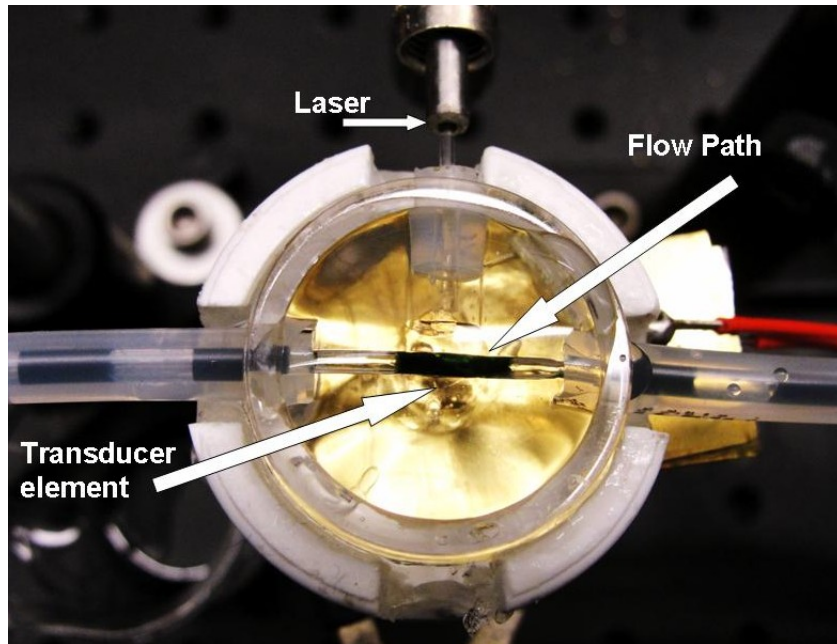


Figure 3.3: Orthogonal View of the Detection Chamber

each wavelength.

## 3.4 Results

### 3.4.1 Pigment Containing Leukocytes

The release of hemozoin into the environment where *P. falciparum* grows is clearly prevalent to any who have cultured this parasite. By microscopically analyzing the cultures, the abundance of this optically absorbing bio-crystal becomes obviously apparent. It can be seen free floating in the cultures, as well as housed within the infected erythrocytes as indicated in Figure 3.4. When cultured with our leukocyte enriched blood, the free hemozoin was ingested by the immunologically active white blood cells as indicated by arrow A in Figure 3.5. This intake by and subsequent isolation of the active white blood cells provided an optically negligible vessel for the transport and excitation of hemozoin that models conditions similar to those found in an infected host.

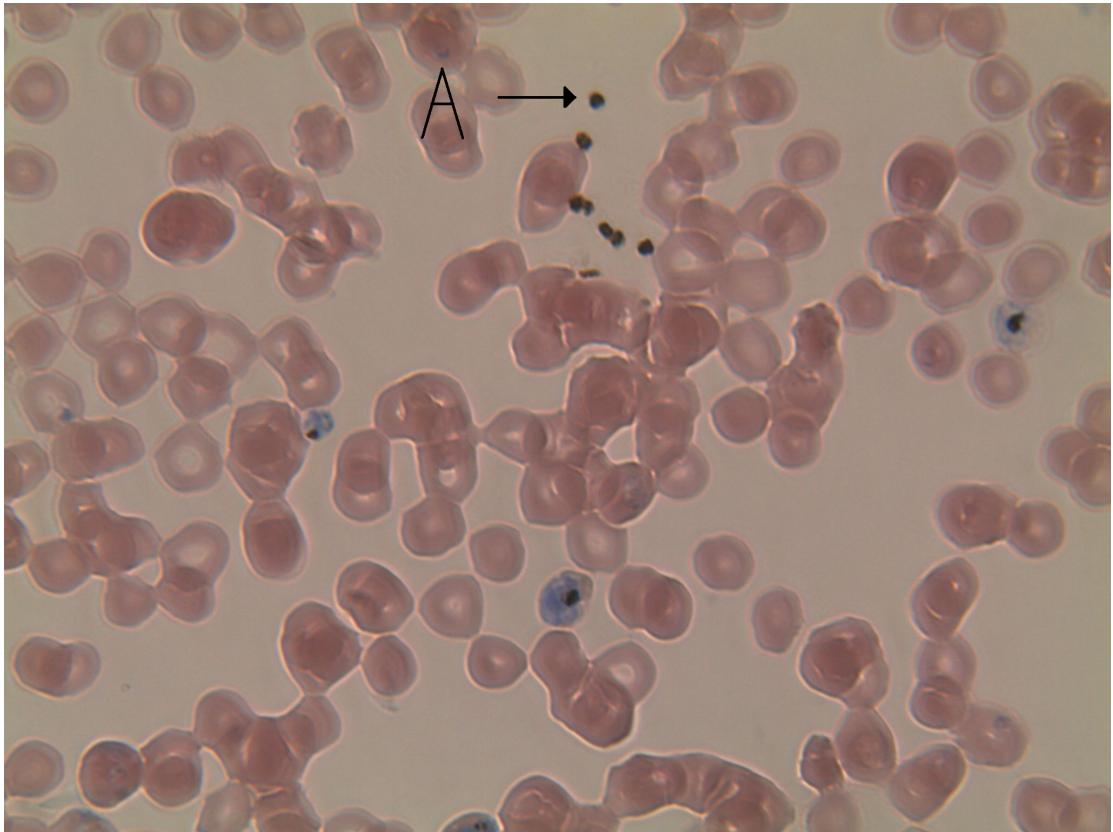


Figure 3.4: Free Hemozoin as Indicated By Arrow



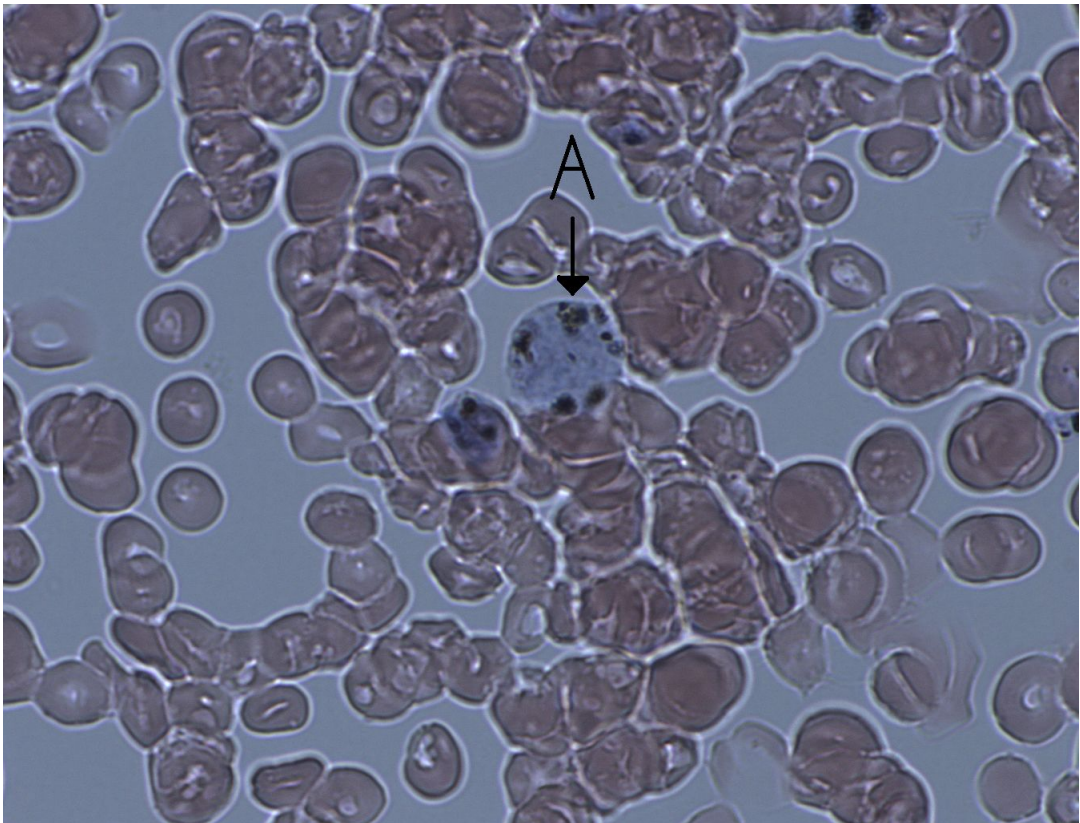


Figure 3.5: Pigment Containing Leukocyte as Indicated By Arrow

### **3.4.2 Two-Phase Photoacoustic Detection and Isolation**

A sample solution of PCLs was input through our two phase flow system. A 2  $\mu\text{L}$  slug was created using the previously described two phase flow system. The slug was excited with a single 530 nm wavelength pulse from the Vibrant II laser system. The photoacoustic response was observed on the Tektronix TDS 2024B oscilloscope and the data was saved to a USB storage device. This photoacoustic waveform was graphed using Kaleidagraph and is shown in Figure 3.6. The slug was then captured on a microscope slide post excitation. The samples were stained with Trypan Blue (Sigma-Aldrich, St. Louis MO) and analyzed with an Olympus 1X70 microscope (Olympus, Waltham MA). The samples were imaged on Metamorph(Molecular Devices Inc., Sunnyvale CA) at 60X magnification utilizing a Hamamatsu ORCA ER C4742-80 camera (Hamamatsu Inc., Bridgewater NJ). The images of this post excitation PCLs are displayed in Figure 3.7.

### **3.4.3 Photoacoustic Spectral Analysis**

The data collected by single phase flow as described earlier was input to Kaleidagraph (Synergy Software, Reading PA) where the peak to peak voltage of each individual photoacoustic waveform was analyzed. The peak to peak response was then normalized by the energy of the laser that had been recorded with the energy meter. The values recorded for each wavelength were then averaged and the standard deviation of the measurements was calculated. The average values were graphed and error bars were created using the aforementioned standard deviation. Figure 3.8 shows these graphed averages.

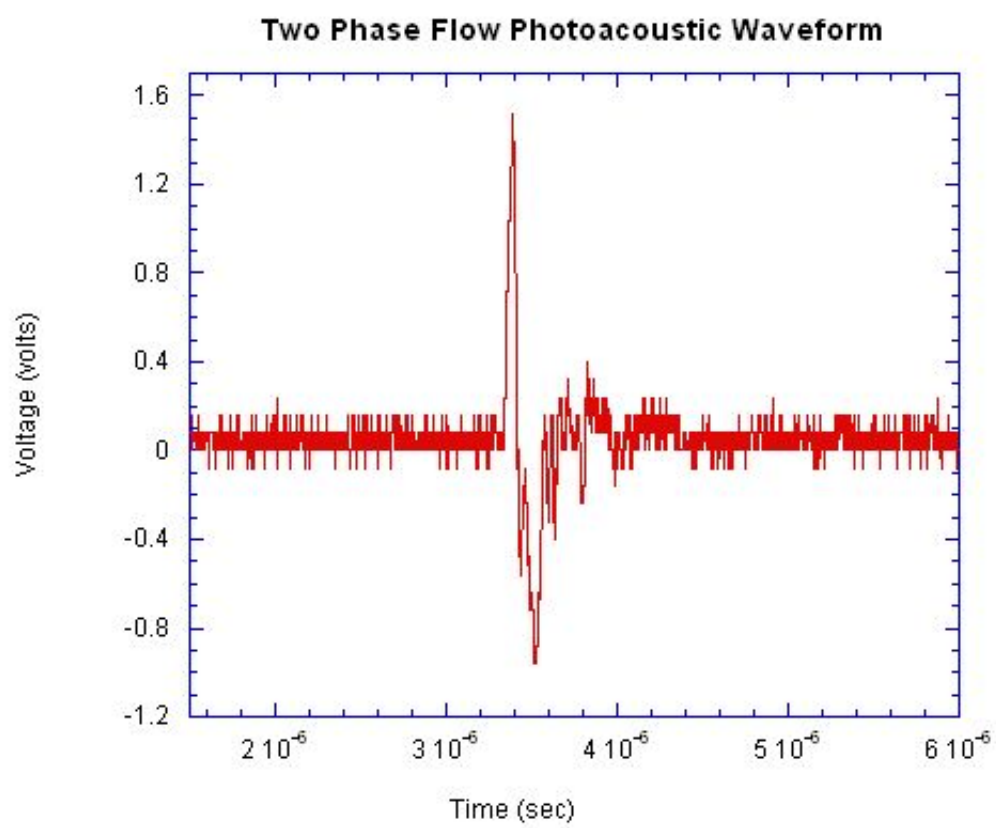


Figure 3.6: 530 nm Photoacoustic Waveform

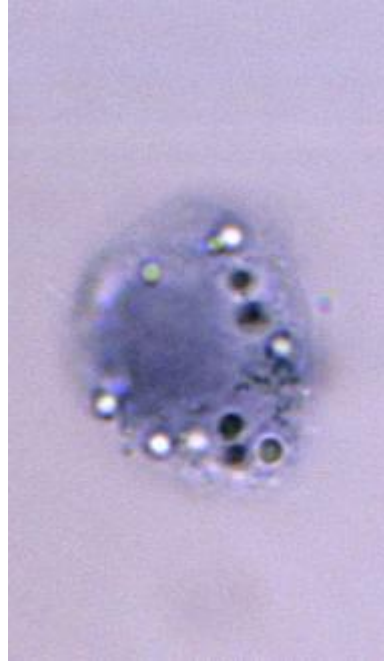


Figure 3.7: Captured Post Excitation PCL

### 3.5 Discussion

A protocol for cultivating *P. falciparum* along with immunologically active white blood cells has not existed prior to our work. While our method for obtaining hemozoin laden leukocytes is functional with an efficacy of  $\sim 90\%$ , there were many failed trials that lead to our current protocol. By culturing *in vitro*, the intrinsic factors of *in vivo* biology should be eliminated. However, we have found that growth rate and infection rate of parasites *in vitro* can vary greatly, causing culture loss due to rampant cell growth. When the concentration of parasites within the culture (parasitemia) exceeds 5%, stability of the culture is lost. This can result in the crash of a culture, in which the parasites and other cells die. Furthermore, the leukocytes do not survive for extended periods of time in the environment that is designed for *P. falciparum* to flourish. Many times the leukocytes died unexpectedly if cultures were allowed to exceed 48 hours of incubation. In order to create a more stable

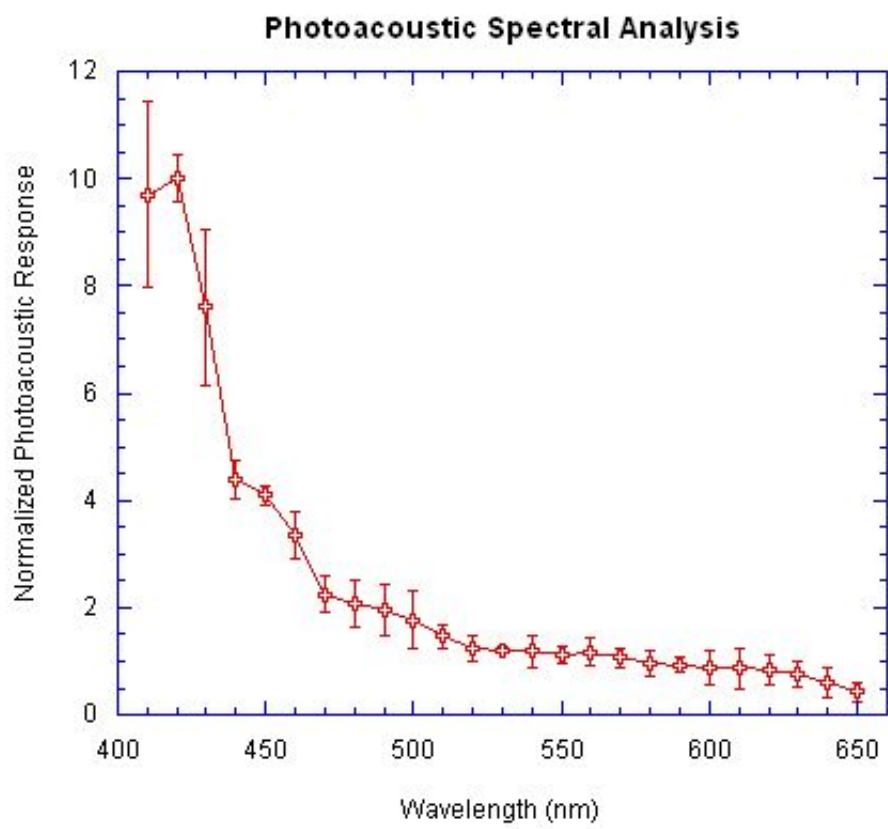


Figure 3.8: Photoacoustic Spectral Analysis

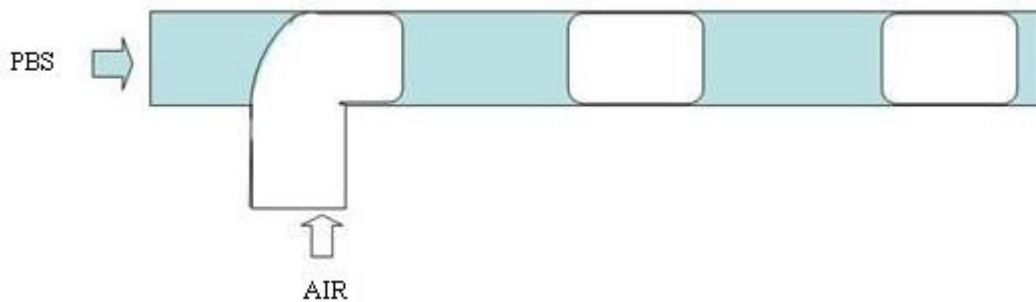


Figure 3.9: Combining Two Immiscible Fluids Into One Flow Path in a Microfluidic System

environment where both the parasites and leukocytes can thrive, it was necessary to start the cultures at low parasitic infection levels with the leukocyte enriched blood. Minimally, there could be slight revisions to our current protocols that could better promote cell growth, stability, and repeatability.

Two-phase flow was created using a T-junction, which combines the two separate phases into one flow path while keeping the phases distinct, as shown in Figure 3.9. Multiple phase combinations were investigated. One phase distinction investigated for use in this system was PBS and oil. While PBS and oil are immiscible, the pressure in the system mixed some oil slightly with the slugs. The oil used was not photoacoustically negligible and produced distorted photoacoustic responses. Another phase distinction, which ultimately was the optimal choice, was that of PBS and air. The PBS and water phases were ultimately preferred because the desired water slug could easily be extracted without contamination of the sample with the neighboring phase. However, when using air and water the liquids can build up pressure and cause inconsistent flow. This could be eliminated by the addition of a surfactant to the sample (Garstecki *et al.*, 2006).

Our Sample of PCLs that was input into the system had several marked characteristics that were recorded prior to use in the system. After our culture was isolated and the PCLs were suspended in 6 ml of PBS. A cell count was performed

on a 10  $\mu\text{L}$  sample using a hemocytometer. The sample was mixed with 10  $\mu\text{L}$  of Trypan Blue and input to the hemocytometer. The cell counts showed that the concentration was  $\sim 5000$  cells/ $\mu\text{L}$  of solution. Given that our slugs were 2  $\mu\text{L}$  this puts  $\sim 10000$  cells in our detection area. By microscopic verification, the percentage of white cells containing Hemozoin was  $\sim 90\%$  and in those cells the volume of hemozoin contained was  $\sim 10\%$  of the total cell volume. Given that a sample taken from a patient would have  $\sim 10,000$  cells per  $\mu\text{L}$ , sampling this dilution is going to be less sensitive than cells extracted from a patient. The sample was excited at 530 nm and exhibited a significant photoacoustic response. Post excitation the slug was captured on a microscopic slide and the exciting factor was concluded to be a pigment containing leukocyte that was isolated from our culturing process. Given that leukocytes have a diameter of  $\sim 16$   $\mu\text{m}$  their volume is approximately  $2000$   $\mu\text{m}^3$ . Multiplying by the percentage of laden leukocytes and the amount of hemozoin per leukocyte we can see that the approximate volume of hemozoin contained within our 2  $\mu\text{L}$  slug is .002  $\mu\text{Liters}$ , or .1% of the total solution volume. This indicates that our system is sensitive to very low concentrations of hemozoin.

The photoacoustic spectral analysis shows a marked increase in photoacoustic output near the ultraviolet regime, with a peak near the 410 nm wavelength. This coincides with spectral analysis of hemozoin and other heme based proteins such as  $\beta$ -hematin and hemoglobin (Bohle *et al.*, 1994; Hempelmann & Marques, 1994; Faber *et al.*, 2003). This indicates a wavelength that is highly sensitive to detection of hemozoin in small quantities. Expansion of this knowledge coupled with the use of this technique could also be applied to several other lesser known parasites, such as *Schistosoma Mansoni* and *Rhodnius Prolixus*, that produce similar byproducts (Oliveira *et al.*, 2000a; Oliveira *et al.*, 2005; Oliveira *et al.*, 2000b).

A skilled microscopic analyst can only accurately diagnose malaria with an efficacy of  $\sim 71\%$  (Ohrt *et al.*, 2002), and in many developing countries, microscopy is even less reliable because the microscopists are insufficiently trained. The microscopes and reagents are of poor quality, and often the supply of electricity is unreliable. Furthermore, in non-endemic countries, laboratory technicians are often

unfamiliar with malaria and may miss the parasites (CDC, 2011). Other methods of diagnosis such as antigen detection or molecular diagnosis, are not widely available, expensive, and not accurate enough to be considered reliable methods of diagnosis (CDC, 2011). This leaves a need for detection systems that are accurate, easy to use, and sensitive. Our system has shown to produce strong signals with a .1% hemozoin concentration per volume of solution. Given the size of the photoacoustic response at 410 nm, our system should be able to detect much smaller concentrations. Accurate diagnosis is critical due to an increase in drug resistant parasite strains (Petersen *et al.*, 2011; Hyde, 2005), cost of medication, and devastated symptoms of disease progression.

Future work from our group should include the analysis of blood from infected human malaria patients and animal models. Since malaria is no longer endemic in the United States, these studies may be better suited for application in endemic regions. The existence of a detection system with a high efficacy of true positives and a low chance of false negatives could revolutionize the treatment and diagnosis of malaria in the regions it has the most damaging physical and socioeconomic effects.



# Chapter 4

## General Discussion and Conclusions

### 4.1 Photoacoustic Detection System

The photoacoustic system used for the detection of malaria pigment as a method for diagnosing *P. falciparum* infection has undergone a number of revisions since its original conception. Nearly every aspect of the system has been scrutinized for defects which may have caused diminished responses or undetermined energy readings. The initial well design was changed to a flow chamber in order to decrease the sample volume and increase accuracy of sample density. The energy meter was relocated in order to increase the accuracy of energy recording. The transducer design went through numerous revisions in order to ensure optimal acoustic response while minimizing energy fluctuations and inherent noise. These revisions show that the system is in a constant state of evolution. Even given the modifications to the system that have been made, the future may include more revisions that further increase the viability of detecting malaria byproducts via photoacoustic methods.

The data collected shows strong evidence that this system has the ability to detect hemozoin housed within immunologically active host leukocytes. The device, in its current form, shows more promise of detecting malaria infection than previous incarnations. Once the cells have been cultured and cultivated, the isolation of the pigment containing leukocytes is fairly easy. A simple density centrifugation of a potentially infected patient, or our cultured cells, is all that is required to prepare the samples for testing within the system. The flow system creates a simple effective method for defining small sample sizes that can be tested rapidly and efficiently. The system also has the ability to create a large sample throughput which enables large volumes to be scanned. The sample solutions can be changed quickly and the system

can also be flushed rapidly so that the interval between testing multiple samples is minimized.

While further modifications to the system may yield improvement in the aforementioned areas, the current methods used in our detection system appear to create a system which is best suited to scan large volumes of solution while maintaining a high sensitivity to the presence of hemozoin.

## 4.2 Pigment Containing Leukocyte Detection

The photoacoustic system has successfully detected malaria byproducts housed within human leukocytes. While performing our spectroscopic analysis of the pigment containing leukocytes we detected the presence of hemozoin across the visible spectrum, and given the magnitude of our responses around the ultraviolet regime we can infer that our system will be able to detect much smaller concentrations of hemozoin at these wavelengths. Given that our system has successfully detected concentrations of .1% hemozoin per total volume with responses upwards of 8 volts peak to peak and given that we can differentiate response in the millivolt range, we may even be able to detect signals from a single infected cell. This would be significantly greater than the effective diagnostic range of traditional microscopic detection methods.

While currently we can not differentiate the photoacoustic waveform created from hemozoin to that of other absorbers, there is evidence to show that further experimentation can give us the information needed to do so. By performing concentration experimentation to properly determine the absorption coefficient we should be able to successfully distinguish the waveform created by hemozoin from those created by other blood born absorbers such as hemoglobin and metastatic melanoma.

## 4.3 Future Directions

A substantial amount of work remains before the proposed detection system can be implemented in a clinical setting. While there is strong evidence supporting the efficacy of the system, human and animal studies have yet to be implemented. Having performed substantial amounts of work with the biological culturing of the parasites, I have learned that certain biological factors can greatly complicate situations. We can infer from our results that the system will detect hemozoin as expected. However, while the system performs as expected with cultured samples, the introduction of human or animal samples to the system may create unforeseen hurdles to the completion of the project.

While obtaining blood from an infected human would prove quite difficult in the United States, an animal model could be the next step in solidifying the successfulness of our system. By performing experiments with animal models we can prove the efficacy of the system within live subjects, as opposed to obtaining samples through artificial means. This would show that our system works with the actual progression of the disease. We could show how quickly we can detect the presence of malaria post infection and compare our results to microscopic diagnosis. This would also be a stepping stone towards testing human patients.

There are other avenues that have been yet to be explored as well. Nanoparticle tagging for example. The affinity of free hemozoin for the tagging of particles has not been explored. Quantum dots and other nanoparticles have been shown to increase photoacoustic sensitivity and are a possible vector for future research.

## 4.4 Conclusion

Our photoacoustic detection system has proven successful for our cultured cells. If our success so far translates into human trials, we will have developed the most sensitive method for malaria detection to date. By possessing the ability to examine samples without the use of trained microscopic analysts, our photoacoustic detection system could revolutionize the way we diagnose malaria. Though startup costs

remain an issue, the amount of time and money conserved from the deployment of our system would more than make up for the initial cost.

We have also provided a novel method for culturing living parasites in conjunction with immunologically active human leukocytes. This breakthrough could be applied to other disease studies, or further applied to the study of malaria. It was a significant hurdle to overcome in the process of developing our photoacoustic system. The isolation of the immunologically active leukocytes that have been in the presence of active disease agents could prove to be useful in the study of numerous infectious agents.

The benefits of our system have been presented and are clearly evidenced by our results. While drawbacks are still present, we have shown how this system could impact the malaria stricken community. Malaria afflicts more people than any other infectious agent on this planet. Hopefully our system will lead to more accurate timely diagnosis, and aid in the treatment of this disease.

# BIBLIOGRAPHY

Agarwal, A., Huang, SW, ODonnell, M., Day, KC, Day, M., Kotov, N., & Ashkenazi, S. 2007. Targeted gold nanorod contrast agent for prostate cancer detection by photoacoustic imaging. *Journal of Applied Physics*, **102**, 064701.

Balasubramanian, D., Mohan Rao, C., & Panijpan, B. 1984. The malaria parasite monitored by photoacoustic spectroscopy. *Science*, **223**(4638), 828.

Bell, A.G. 1881. *Upon the Production of Sound by Radiant Energy*. New York: Gibson Brothers Printing.

Bohle, D.S., Conklin, B.J., Cox, D., Madsen, S.K., Paulson, S., Stephens, P.W., & Yee, G.T. 1994. Structural and Spectroscopic Studies of b-Hematin (the Heme Coordination Polymer in Malaria Pigment). *Pages 497–518 of: ACS Symposium Series*, vol. 572. ACS Publications.

CDC. 2011. *Frequently Asked Questions About Malaria*. Centers for Disease Control <http://www.cdc.gov/malaria/about/faqs.html>.

Clark, H. C., & Tomlinson, W. J. 1949. The pathologic anatomy of malaria. *Malariaology*, **2**(874).

Faber, D.J., Mik, E.G., Aalders, M.C.G., & van Leeuwen, T.G. 2003. Light absorption of (oxy-) hemoglobin assessed by spectroscopic optical coherence tomography. *Optics Letters*, **28**(16), 1436–1438.

Garstecki, P., Fuerstman, M.J., Stone, H.A., & Whitesides, G.M. 2006. Formation of droplets and bubbles in a microfluidic T-junction: scaling and mechanism of break-up. *Lab on a Chip*, **6**(3), 437–446.

Gupta, A., & Kumar, R. 2010. Effect of geometry on droplet formation in the squeezing regime in a microfluidic T-junction. *Microfluidics and Nanofluidics*, **8**(6), 799–812.

Hempelmann, E., & Marques, H.M. 1994. Analysis of malaria pigment from *Plasmodium falciparum*. *Journal of Pharmacological and Toxicological Methods*, **32**(1), 25–30.

Hoelen, CGA, De Mul, FFM, Pongers, R., & Dekker, A. 1998. Three-dimensional photoacoustic imaging of blood vessels in tissue. *Optics Letters*, **23**(8), 648–650.

Houghton Mifflin's The American Heritage Stedman's Medical Dictionary, Second Edition. 2005. *Blood*. <http://columbia.thefreedictionary.com/blood>.

Hyde, J.E. 2005. Drug-resistant malaria. *Trends in Parasitology*, **21**(11), 494–498.

- Jani, D., Nagarkatti, R., Beatty, W., Angel, R., Slebodnick, C., Andersen, J., Kumar, S., & Rathore, D. 2008. HDPa novel heme detoxification protein from the malaria parasite. *PLoS Pathogens*, **4**(4).
- Joy, D.A., Feng, X., Mu, J., Furuya, T., Chotivanich, K., Krettli, A.U., Ho, M., Wang, A., White, N.J., Suh, E., *et al.* 2003. Early origin and recent expansion of *Plasmodium falciparum*. *Science*, **300**(5617), 318.
- Kolkman, R.G.M., Hondebrink, E., Steenbergen, W., & de Mul, F.F.M. 2003. In vivo photoacoustic imaging of blood vessels using an extreme-narrow aperture sensor. *Selected Topics in Quantum Electronics, IEEE Journal of*, **9**(2), 343–346.
- Krafts, KP, Hempelmann, E., & Oleksyn, B.J. 2011. The color purple: from royalty to laboratory, with apologies to Malachowski. *Biotechnic & Histochemistry*, **86**(1), 7–35.
- Ljungstrom, I., Moll, K., Perlmann, H., Scherf, A., Wahlgren, M., & BioMalPar. 2008. *Methods in malaria research*. MR4/ATCC.
- Milne, LM, Kyi, MS, Chiodini, PL, & Warhurst, DC. 1994. Accuracy of routine laboratory diagnosis of malaria in the United Kingdom. *Journal of Clinical Pathology*, **47**(8), 740.
- Nguyen, PH, Day, N., Pram, TD, Ferguson, DJ, & White, NJ. 1995. Intraleucocytic malaria pigment and prognosis in severe malaria. *Transactions of the Royal Society of Tropical Medicine and Hygiene*, **89**(2), 200.
- Nye, ER. 2002. Alphonse Laveran (1845-1922): discoverer of the malarial parasite and Nobel laureate, 1907. *Journal of Medical Biography*, **10**(2), 81.
- Nye, E.R., & Gibson, M.E. 1997. *Ronald Ross: malarialogist and polymath: a biography*. New York: Macmillan Press Ltd.
- O'Brien, C., Mosley, J., Goldschmidt, B.S., & Viator, J.A. 2010. Detection and capture of single circulating melanoma cells using photoacoustic flowmetry. *Page 75641D of: Proceedings of SPIE*, vol. 7564.
- O'Brien, C.M., Rood, K.D., Gupta, S.K., Mosley, J.D., Goldschmidt, B.S., Sharma, N., Sengupta, S., & Viator, J.A. 2011. Isolation of circulating tumor cells using photoacoustic flowmetry and two phase flow (Proceedings Paper). *In: Proceedings of SPIE*.
- Ohr, C., *et al.* 2002. Impact of microscopy error on estimates of protective efficacy in malaria-prevention trials. *Journal of Infectious Diseases*, **186**(4), 540.
- Oliveira, M.F., D'Avila, J.C.P., Torres, C.R., Oliveira, P.L., Tempone, A.J., Rumjanek, F.D., Braga, C.M.S., Silva, J.R., Dansa-Petretski, M., Oliveira, M.A., *et al.* 2000a. Haemozoin in *Schistosoma mansoni*. *Molecular and Biochemical Parasitology*, **111**(1), 217–222.

- Oliveira, M.F., d'Avila, J.C.P., Torres, C.R., Oliveira, P.L., Tempone, A.J., Rumjanek, F.D., Braga, C.M.S., Silva, J.R., Dansa-Petretski, M., Oliveira, M.A., *et al.* 2000b. Haemozoin in *Schistosoma mansoni*. *Molecular and Biochemical Parasitology*, **111**(1), 217–222.
- Oliveira, M.F., Kycia, S.W., Gomez, A., Kosar, A.J., Rumjanek, D.S., Hempelmann, E., Menezes, D., Vannier-Santos, M.A., Oliveira, P.L., & Ferreira, S.T. 2005. Structural and morphological characterization of hemozoin produced by *Schistosoma mansoni* and *Rhodnius prolixus*. *FEBS Letters*, **579**(27), 6010–6016.
- Paltauf, G., Schmidt-Kloiber, H., & Guss, H. 1996. Light distribution measurements in absorbing materials by optical detection of laser-induced stress waves. *Applied Physics Letters*, **69**, 1526.
- Petersen, I., Eastman, R., & Lanzer, M. 2011. Drug-Resistant Malaria: Molecular Mechanisms and Implications for Public Health. *FEBS Letters*.
- Poinar, G. 2005. *Plasmodium dominicana* n. sp.(Plasmodiidae: Haemospororida) from Tertiary Dominican amber. *Systematic Parasitology*, **61**(1), 47–52.
- Reiter, P. 2000. From Shakespeare to Defoe: malaria in England in the Little Ice Age. *Emerging Infectious Diseases*, **6**(1), 1.
- Roberts, Larry, & Janovy, John. 2008. *Foundations of Parasitology*. Eighth mcgraw-hill printing edn. New York: Mcgraw-Hill.
- Rosencwaig, A. 1980. *Photoacoustics and Photoacoustic Spectroscopy*. New York: Wiley New.
- Savarino, A., Boelaert, J.R., Cassone, A., Majori, G., & Cauda, R. 2003. Effects of chloroquine on viral infections: an old drug against today's diseases. *The Lancet Infectious Diseases*, **3**(11), 722–727.
- Thorsen, T., Roberts, R.W., Arnold, F.H., & Quake, S.R. 2001. Dynamic pattern formation in a vesicle-generating microfluidic device. *Physical Review Letters*, **86**(18), 4163–4166.
- Tice, J.D., Lyon, A.D., & Ismagilov, R.F. 2004. Effects of viscosity on droplet formation and mixing in microfluidic channels. *Analytica Chimica Acta*, **507**(1), 73–77.
- Uhlemann, A.C., & Krishna, S. 2005. Antimalarial multi-drug resistance in Asia: mechanisms and assessment. *Malaria: Drugs, Disease and Post-genomic Biology*, 39–53.
- Viator, J.A., Au, G., Paltauf, G., Jacques, S.L., Prael, S.A., Ren, H., Chen, Z., & Nelson, J.S. 2002. Clinical testing of a photoacoustic probe for port wine stain depth determination. *Lasers in Surgery and Medicine*, **30**(2), 141–148.

- Viator, J.A., Komadina, J., Svaasand, L.O., Aguilar, G., Choi, B., & Nelson, J.S. 2004. A comparative study of photoacoustic and reflectance methods for determination of epidermal melanin content. *Journal of Investigative Dermatology*, **122**(6), 1432–1439.
- Weight, R.M., Viator, J.A., Dale, P.S., Caldwell, C.W., & Lisle, A.E. 2006. Photoacoustic detection of metastatic melanoma cells in the human circulatory system. *Optics Letters*, **31**(20), 2998–3000.
- Weight, R.M., Dale, P.S., & Viator, J.A. 2009. Detection of circulating melanoma cells in human blood using photoacoustic flowmetry. *Pages 106–109 of: Engineering in Medicine and Biology Society, 2009. EMBC 2009. Annual International Conference of the IEEE*. IEEE.
- WHO. 2011. *World Malaria Report*. World Health Organization <http://www.who.int/malaria/publications/atoz/9789241563697/en/index.html>.
- Yuan, Z., Wu, C., Zhao, H., & Jiang, H. 2005. Imaging of small nanoparticle-containing objects by finite-element-based photoacoustic tomography. *Optics Letters*, **30**(22), 3054–3056.
- Zucker, J.R. 1996. Changing patterns of autochthonous malaria transmission in the United States: a review of recent outbreaks. *Emerging Infectious Diseases*, **2**(1), 37.